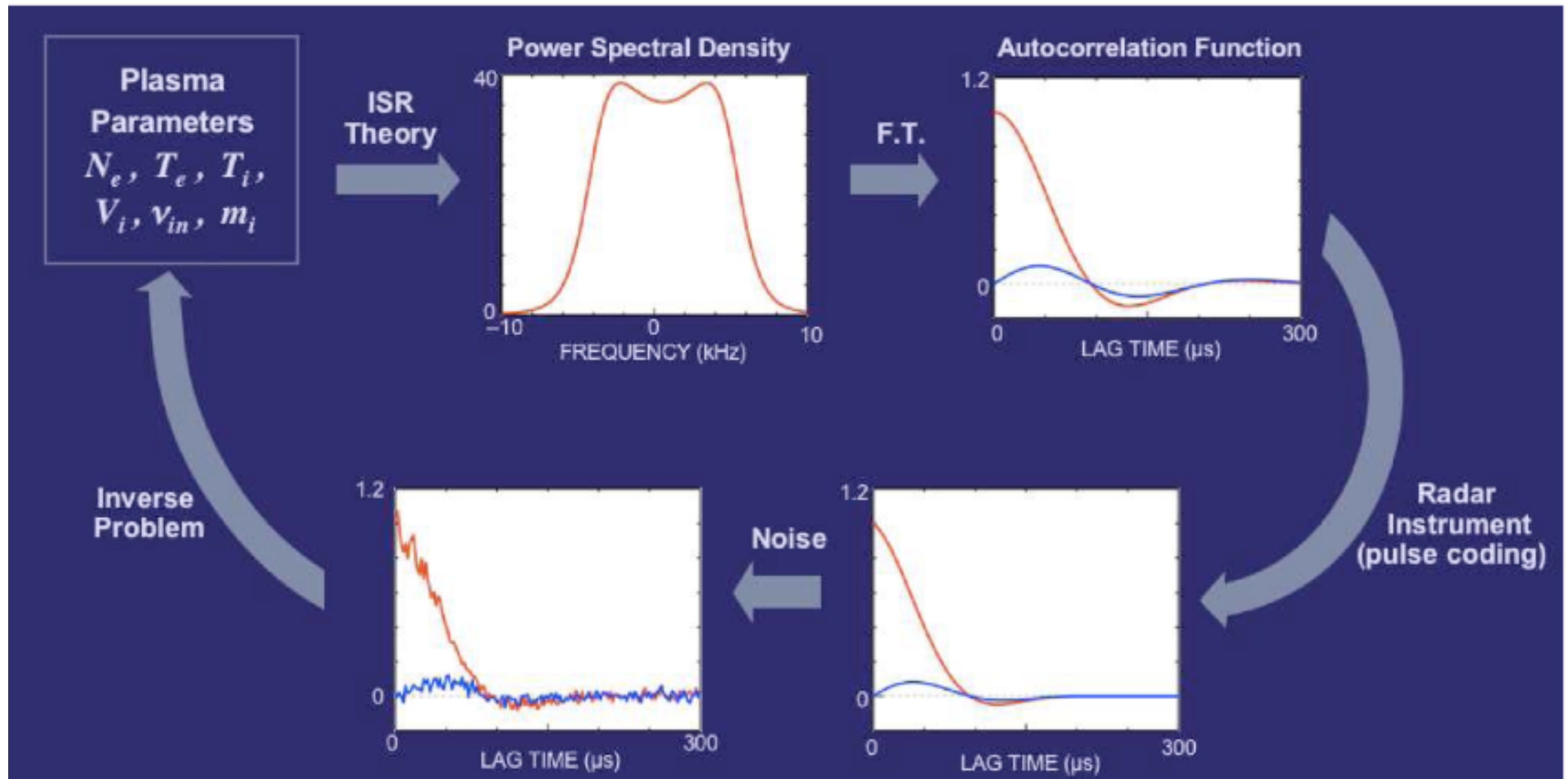


ISR Practicalities: Data Reduction

NB: Power spectrum (freq domain) \leftrightarrow Autocorrelation function (time domain)



Fitting data to a model

Goal: minimize

$$\chi^2 = \sum_{j=1}^n \frac{[y(x_j) - \text{model}(x_j; \vec{p})]^2}{\sigma_j^2}$$

“L2 Norm”

The diagram shows the chi-squared formula with four annotations: 'data' points to the dependent variable $y(x_j)$, 'independent variable' points to x_j , 'parameter vector' points to \vec{p} , and 'uncertainties' points to the denominator σ_j^2 .

Minimize by iterating over parameter vectors.

Some problems are linear least-squares: solvable in one step.

Others are nonlinear least-squares:

model has complicated variations with parameters.

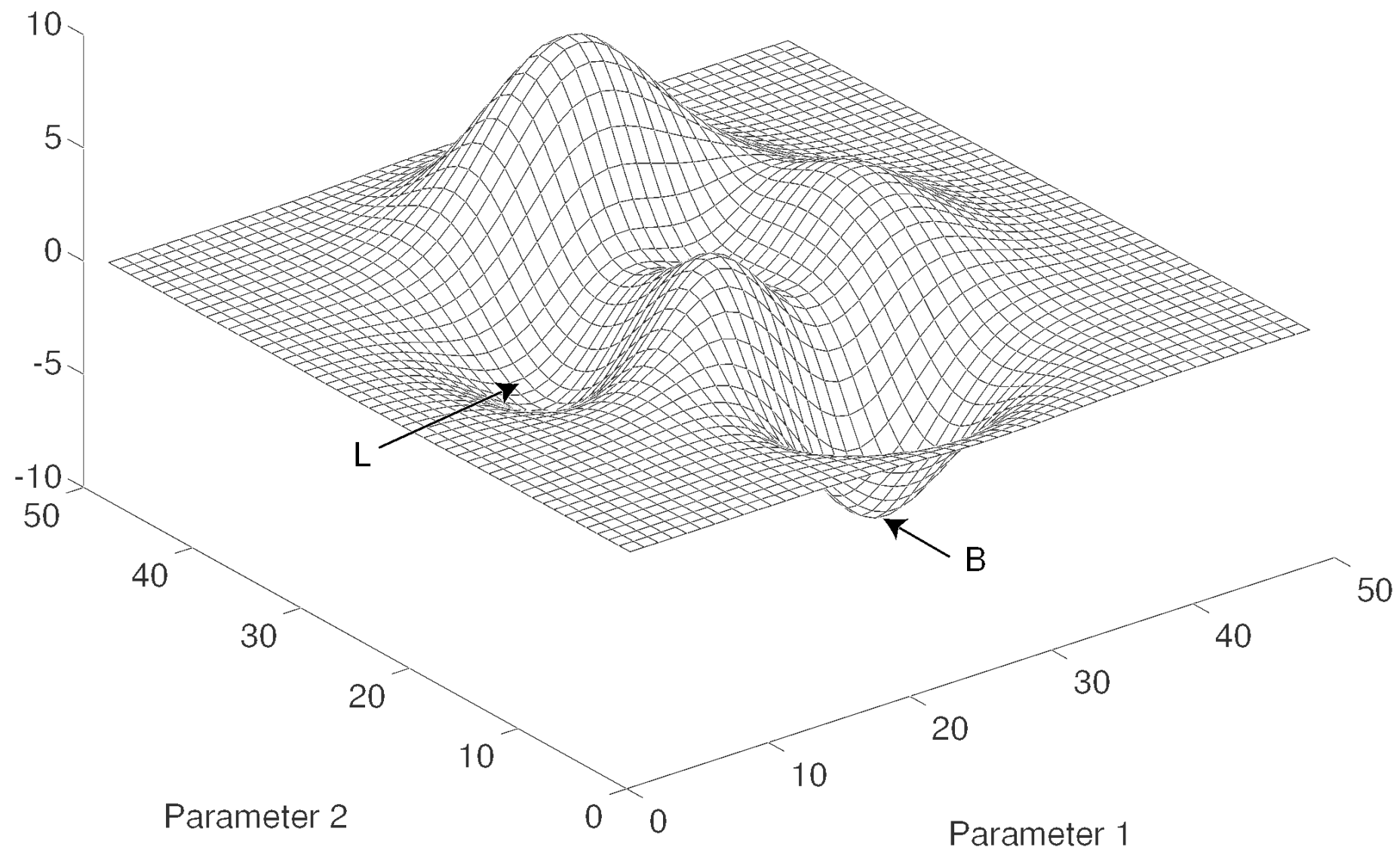
Incoherent scatter is this type.

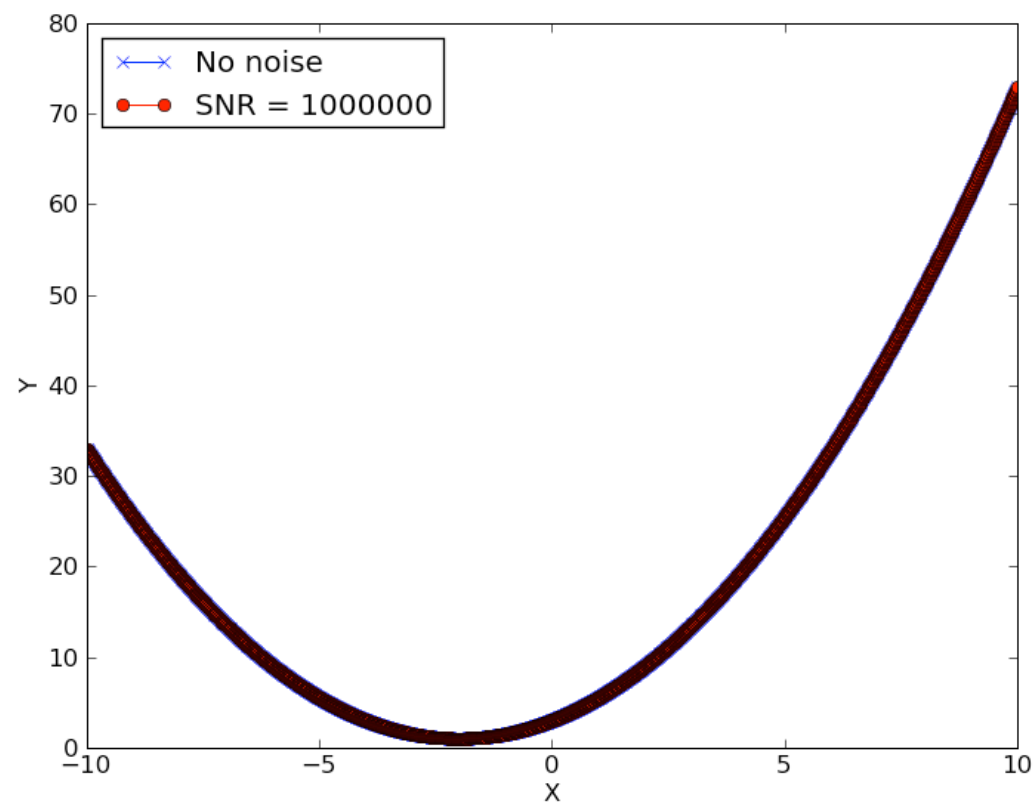
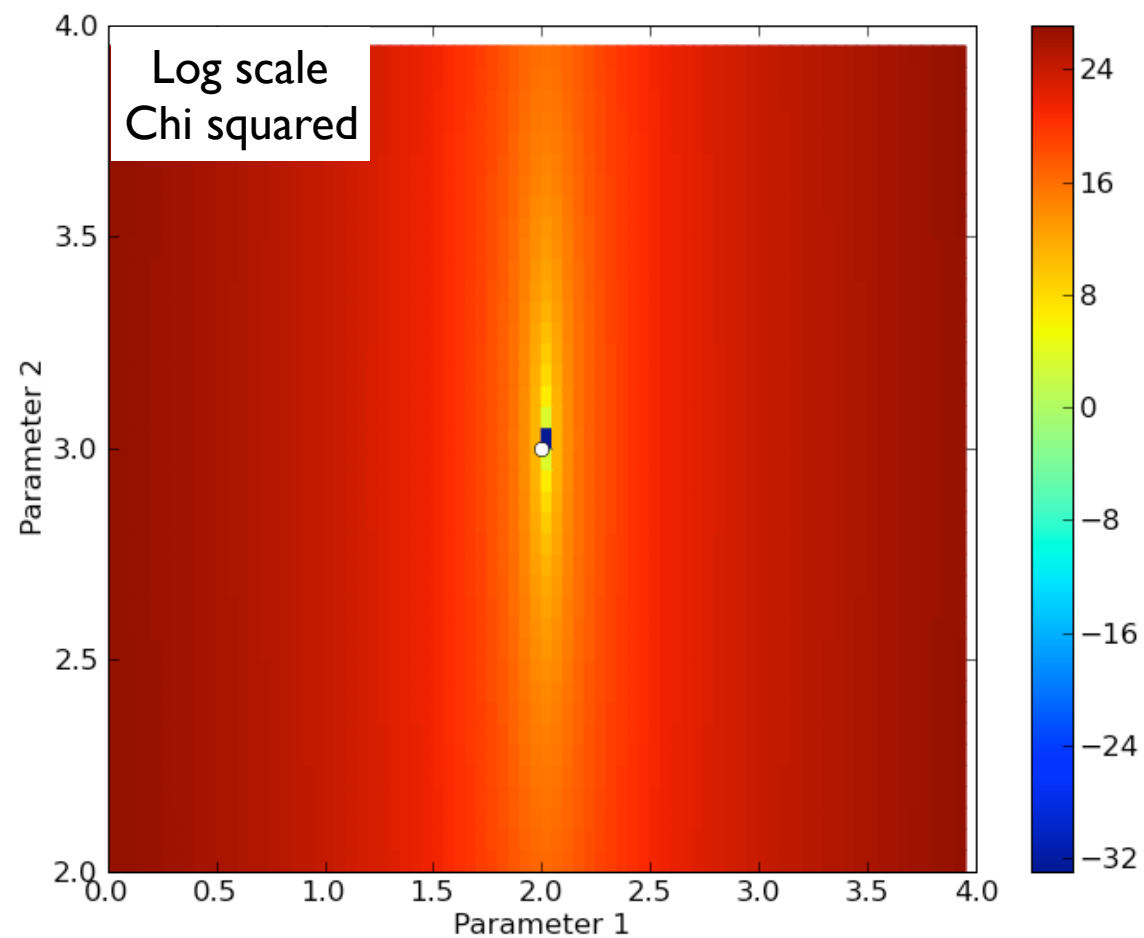
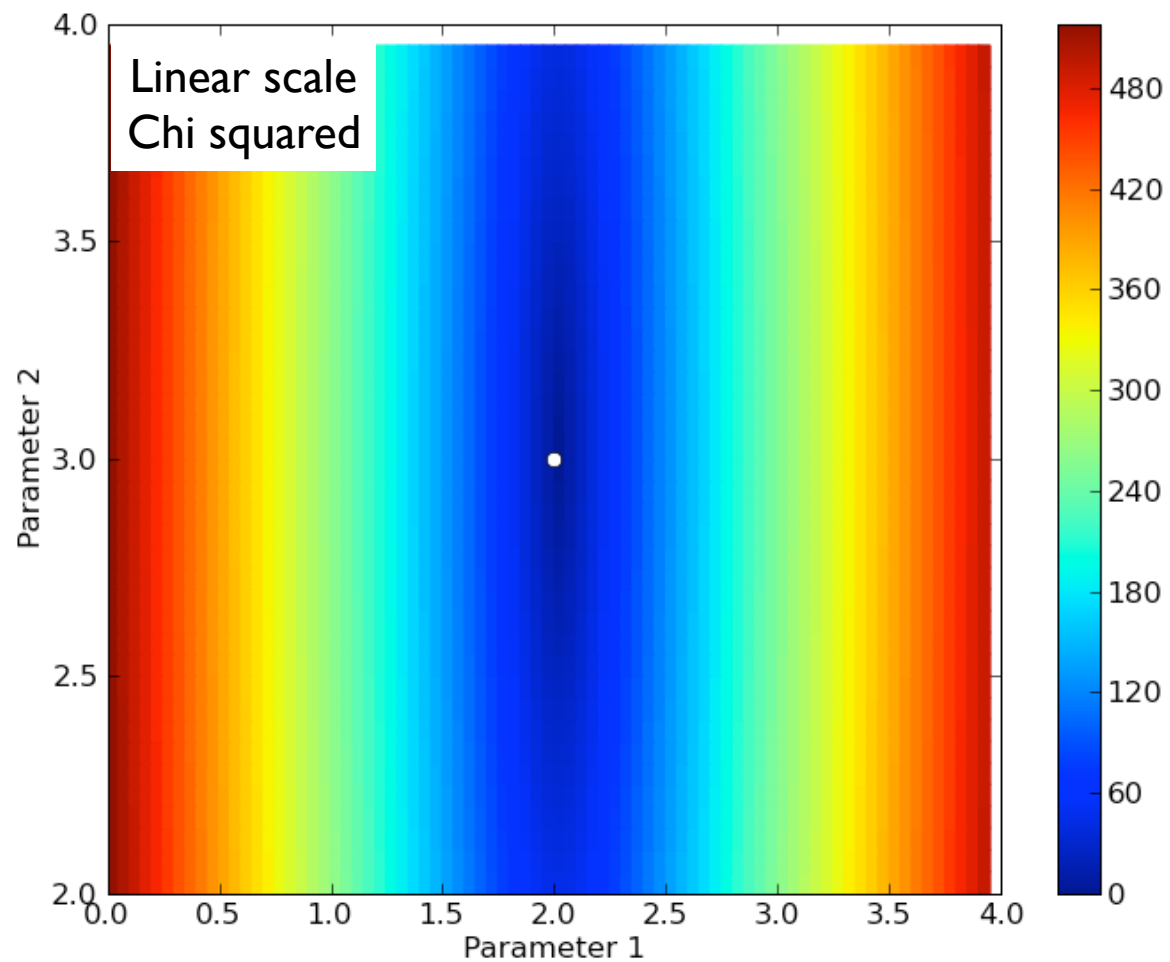
Many different fitting algorithms possible depending on how one analytically expands the minimization function:

- Gradient-search (Nelder-Mead simplex)
- Analytic expansion (parabolic surface)
- Levenberg-Marquardt (balance between gradient and analytic)
- Simulated annealing

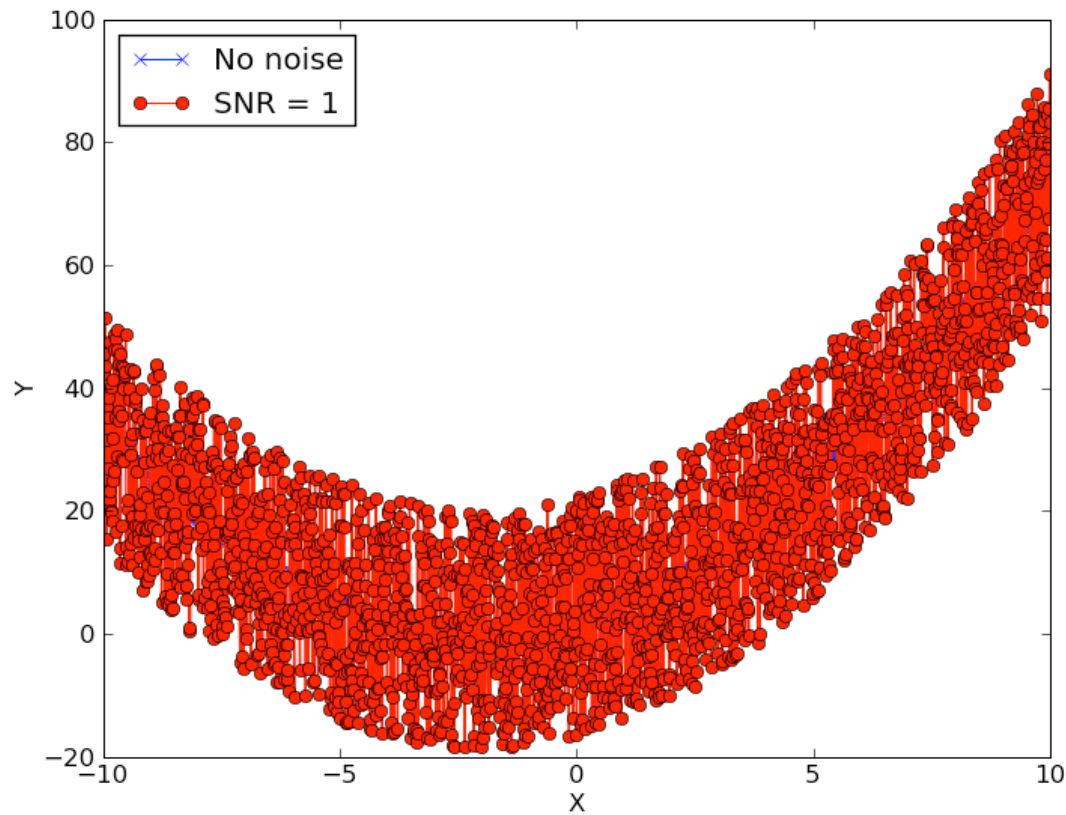
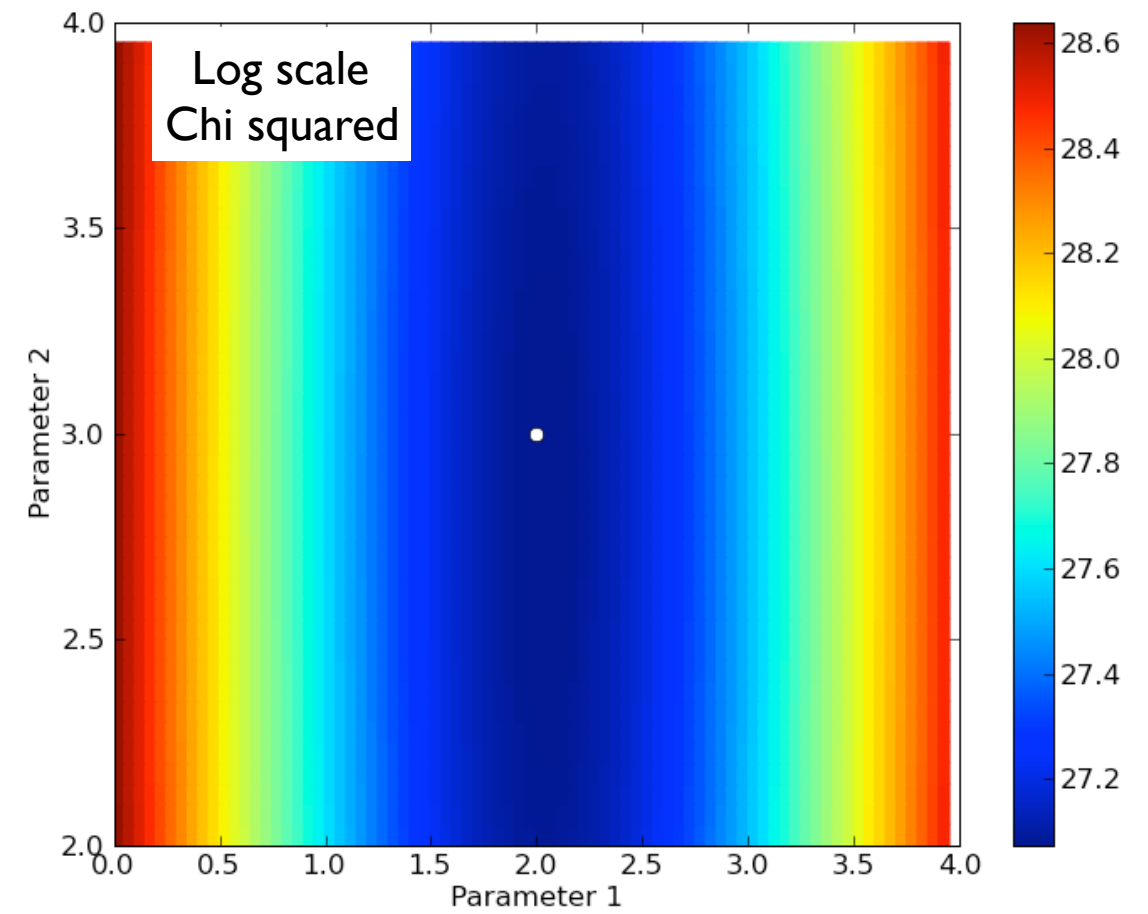
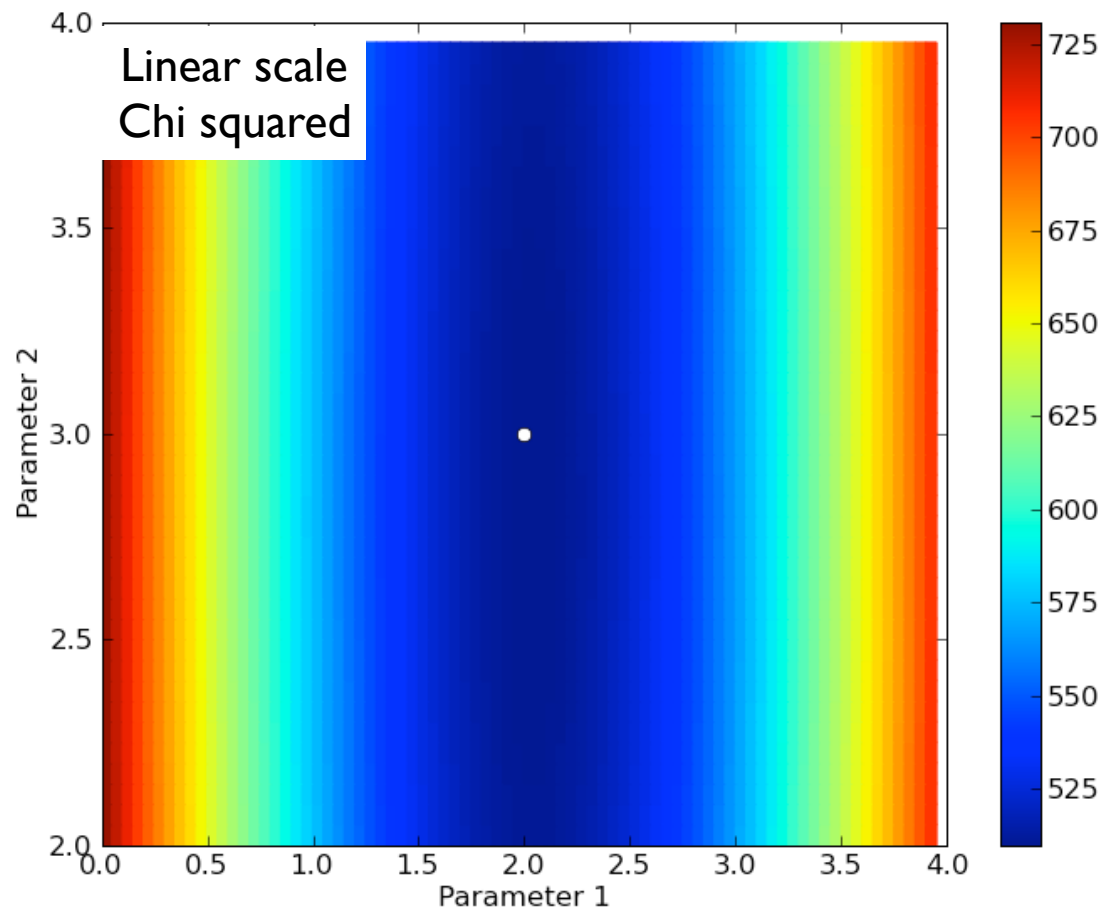
Incoherent Scatter Fit Ambiguities

L, B might both be valid parameter solutions. Might need to use constraints on the parameters to decide which one.

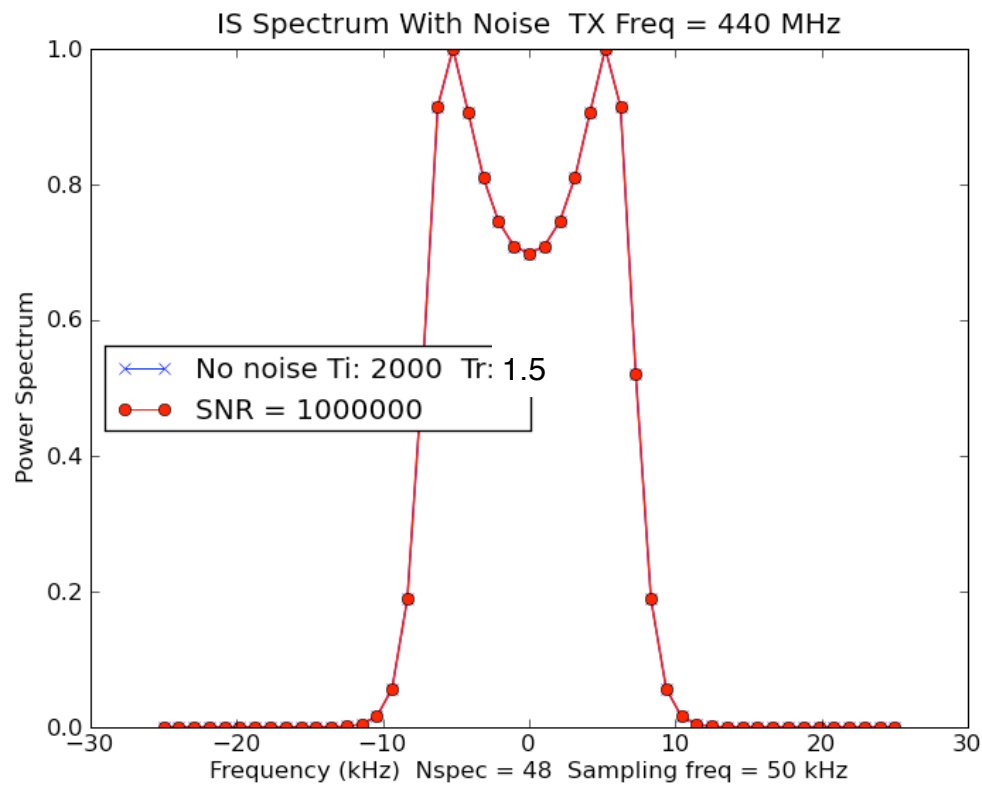
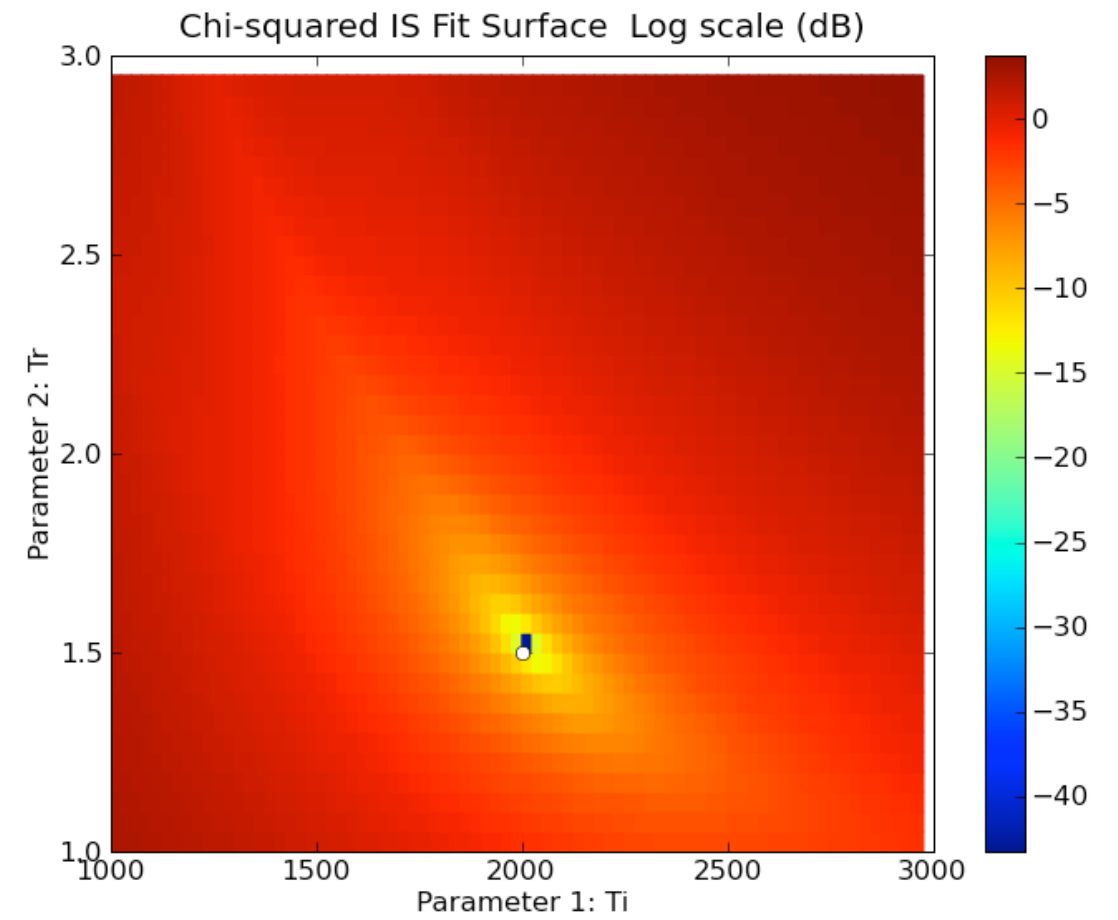
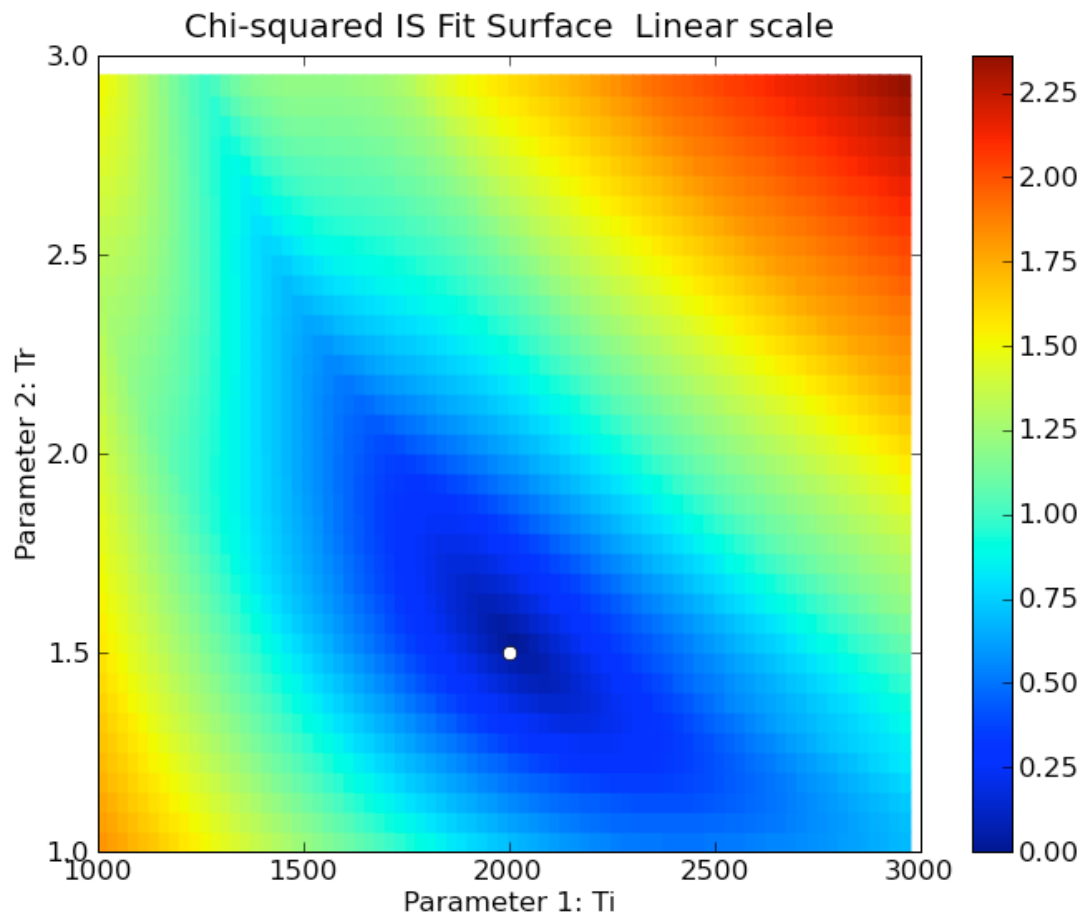




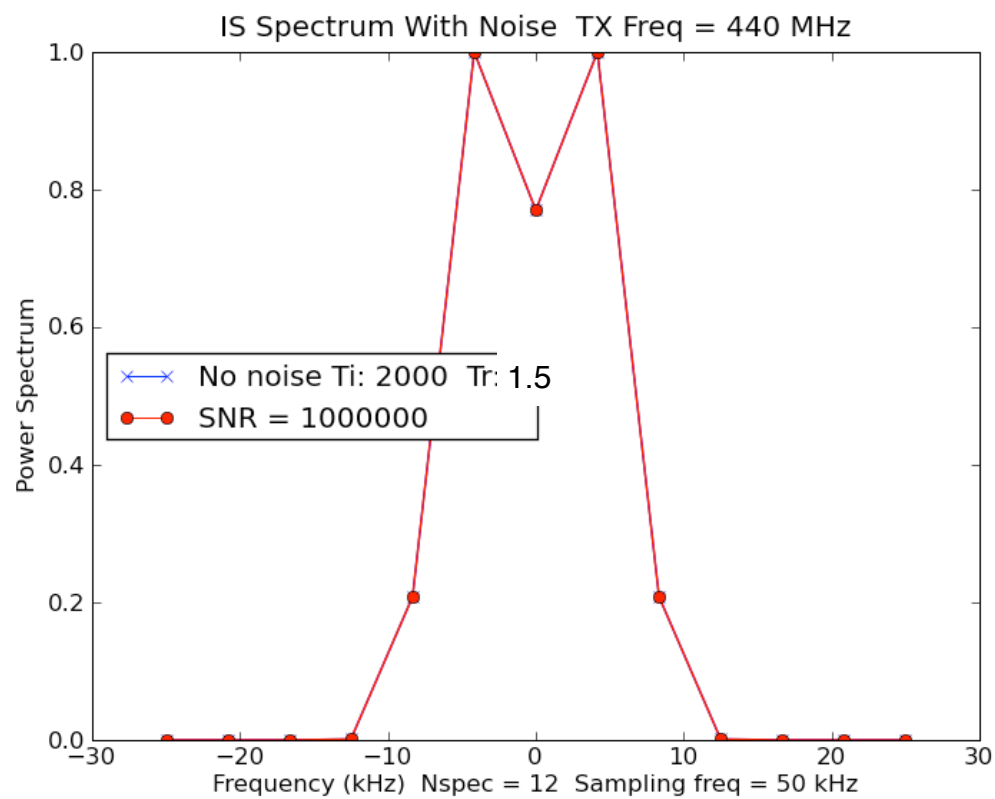
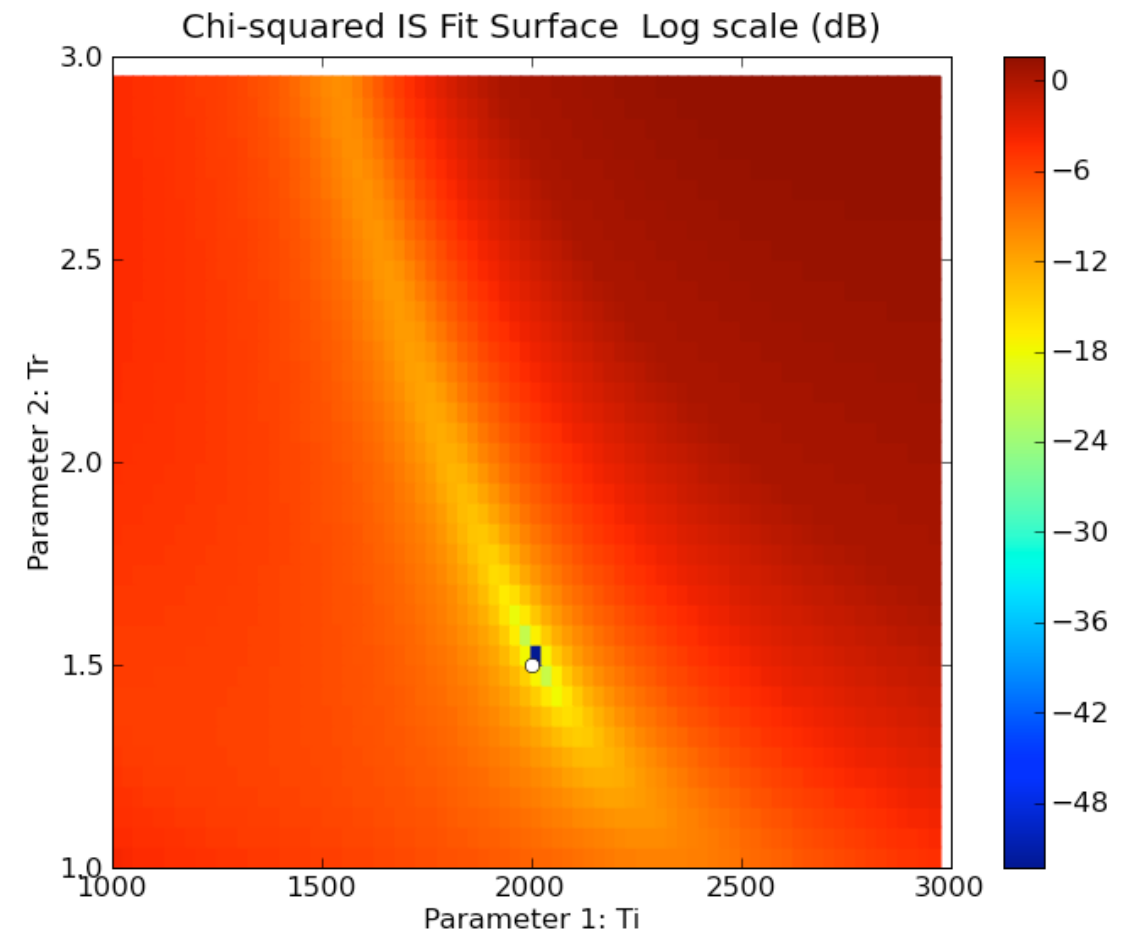
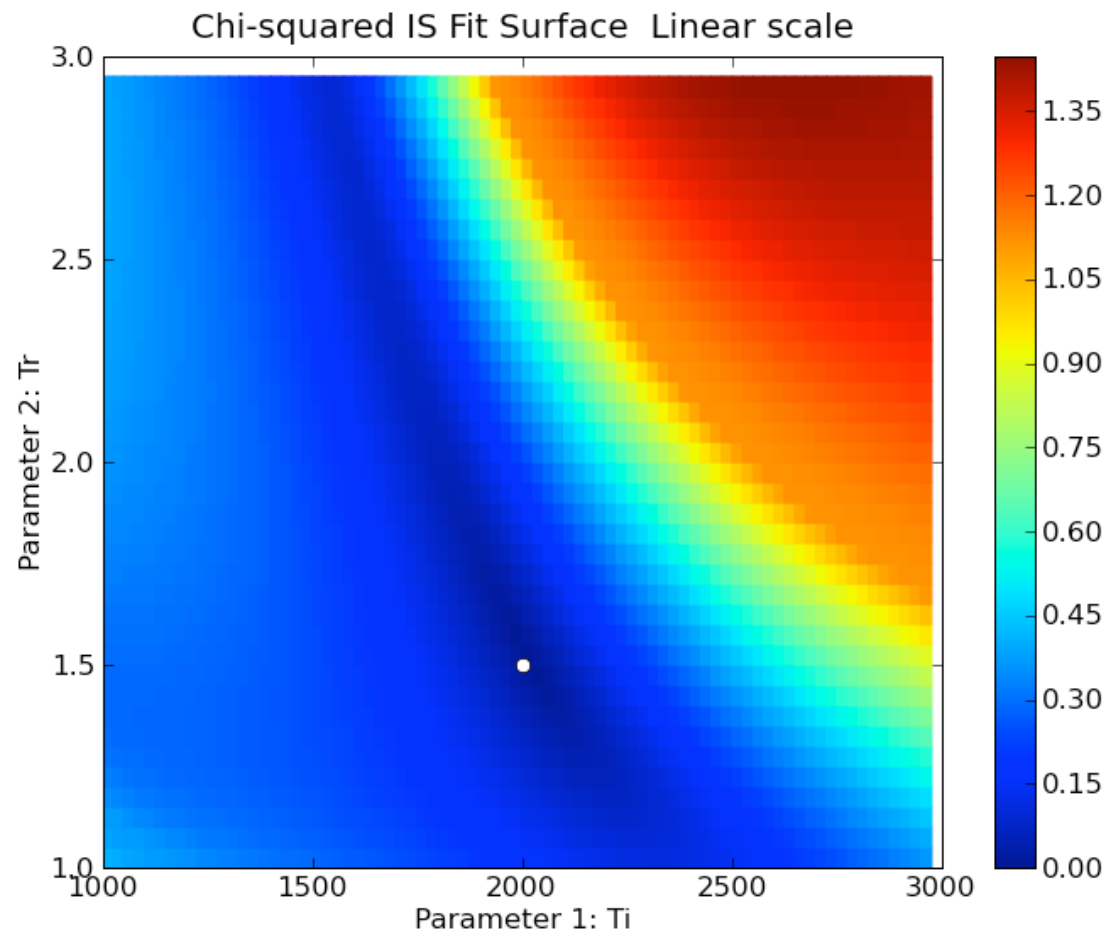
Parabola
 $y = 0.5 x^2 + 2 x + 3$
 Slope, intercept fit
 No noise



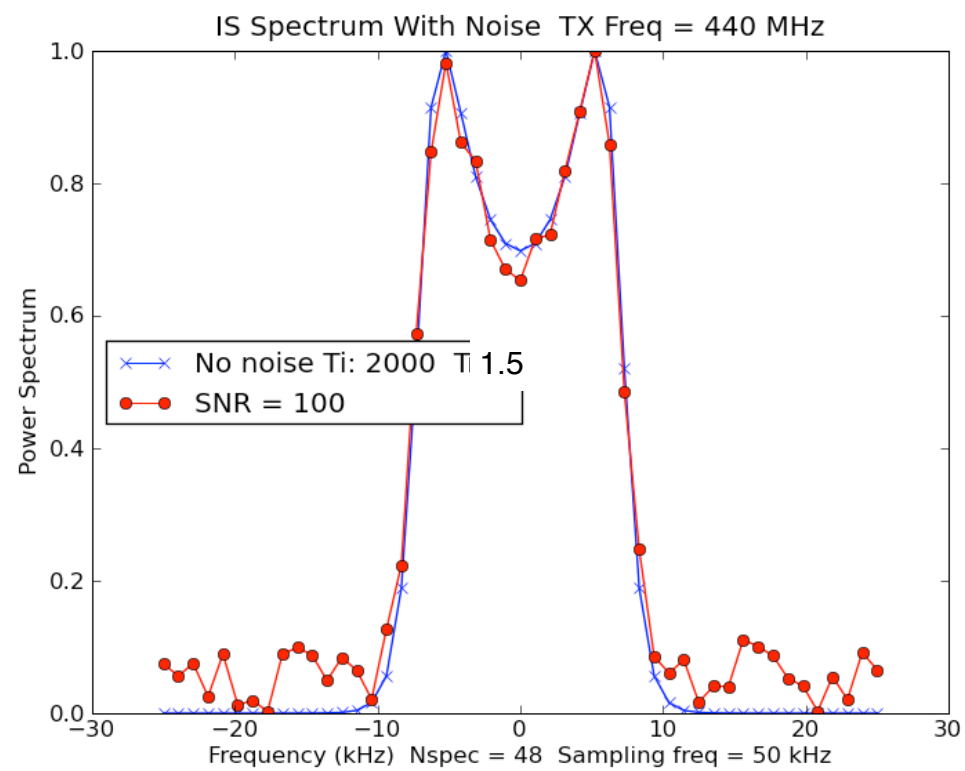
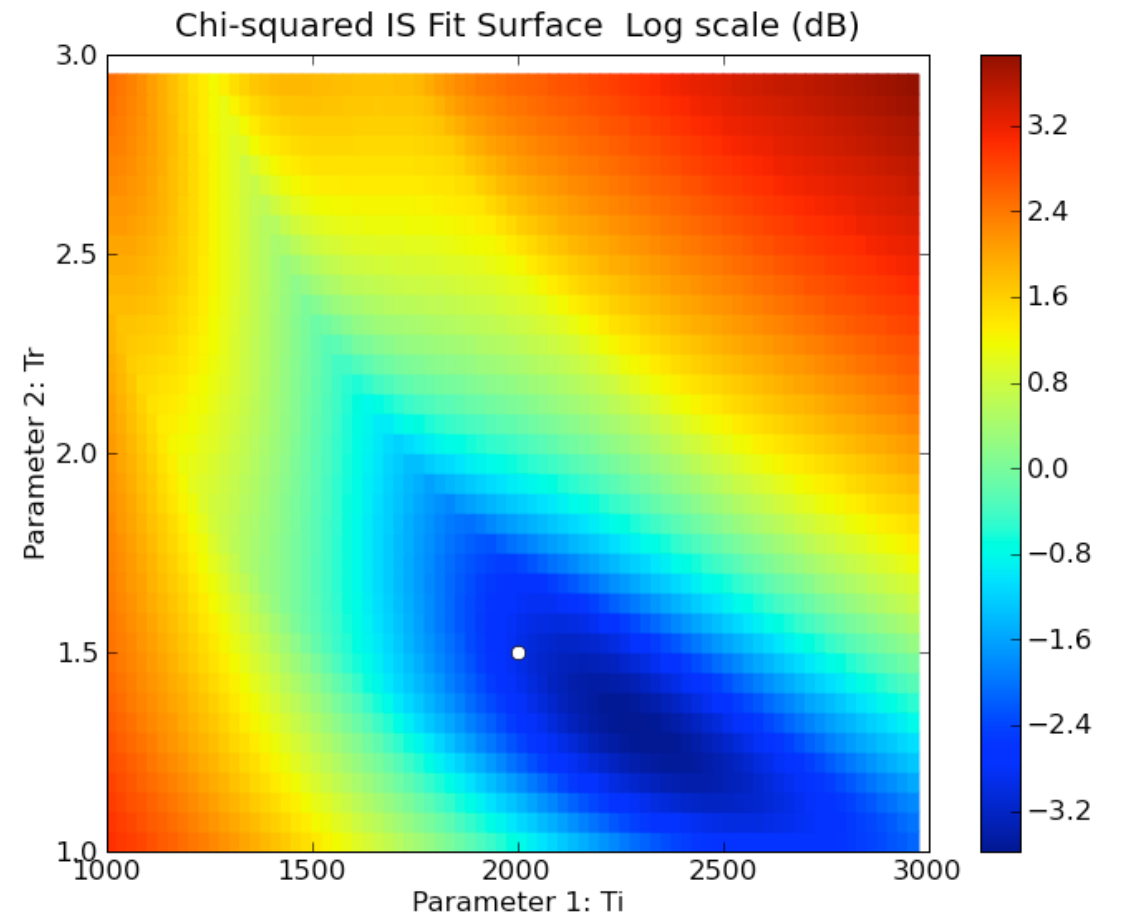
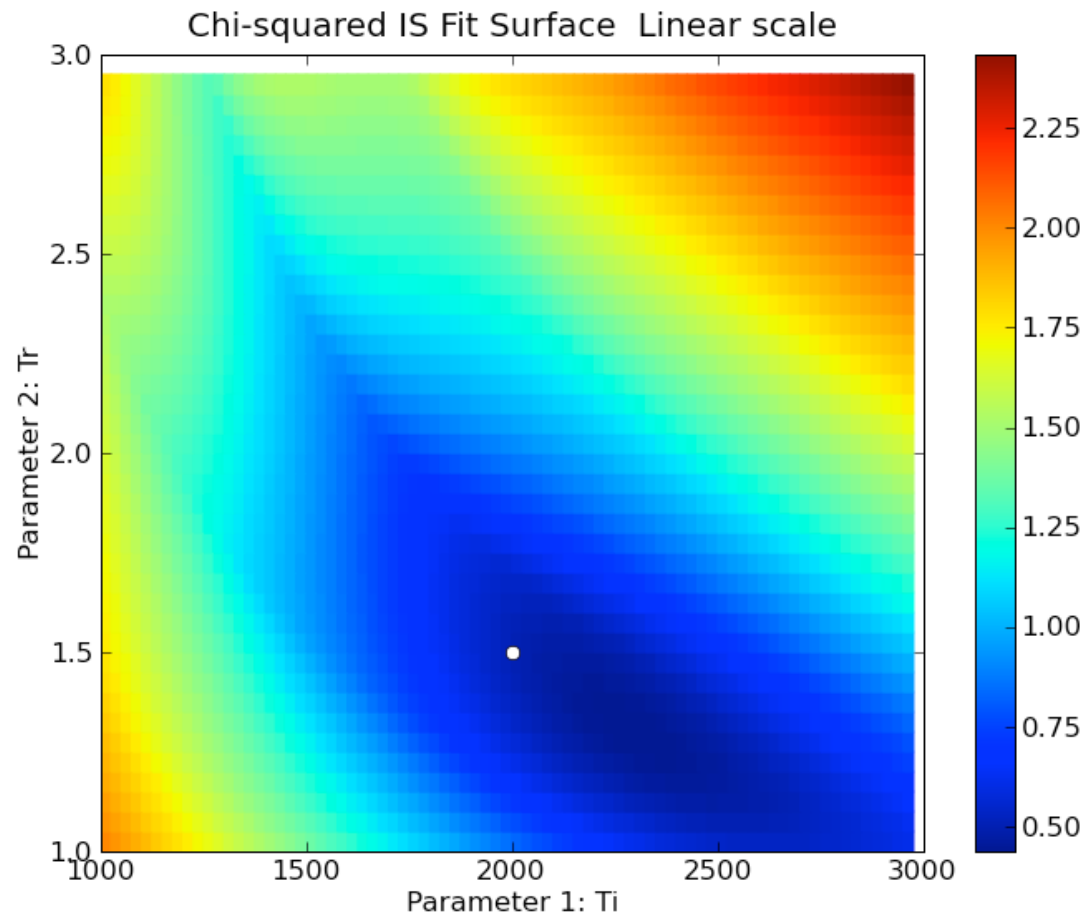
Parabola
 $y = 0.5 x^2 + 2 x + 3$
 Slope, intercept fit
 Noisy



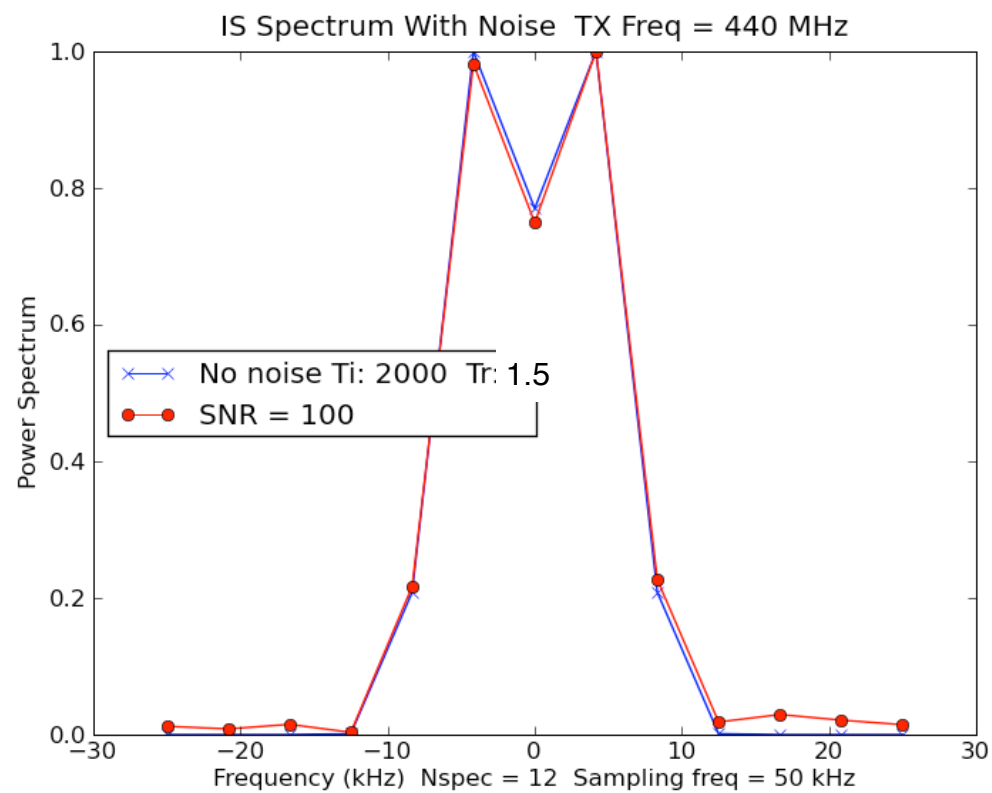
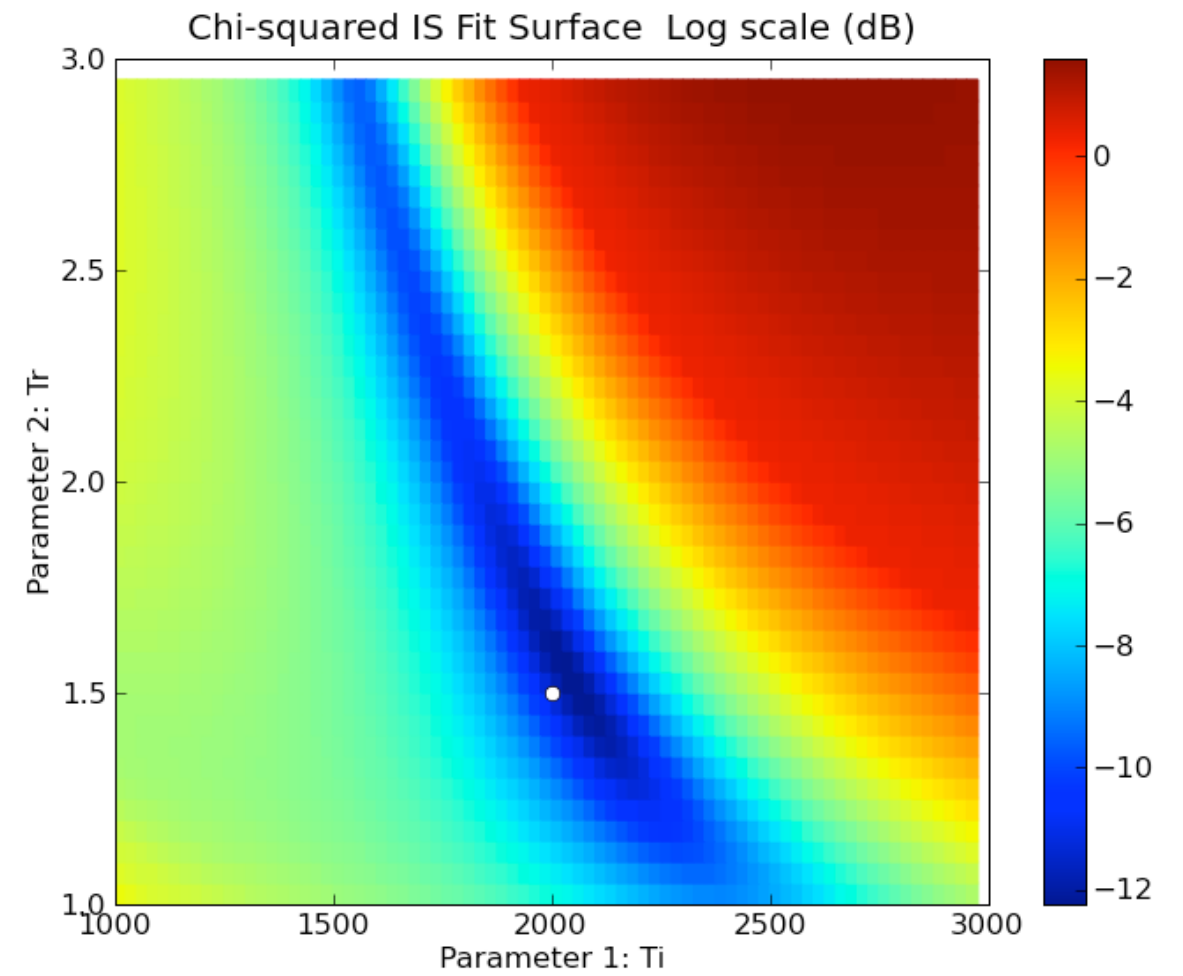
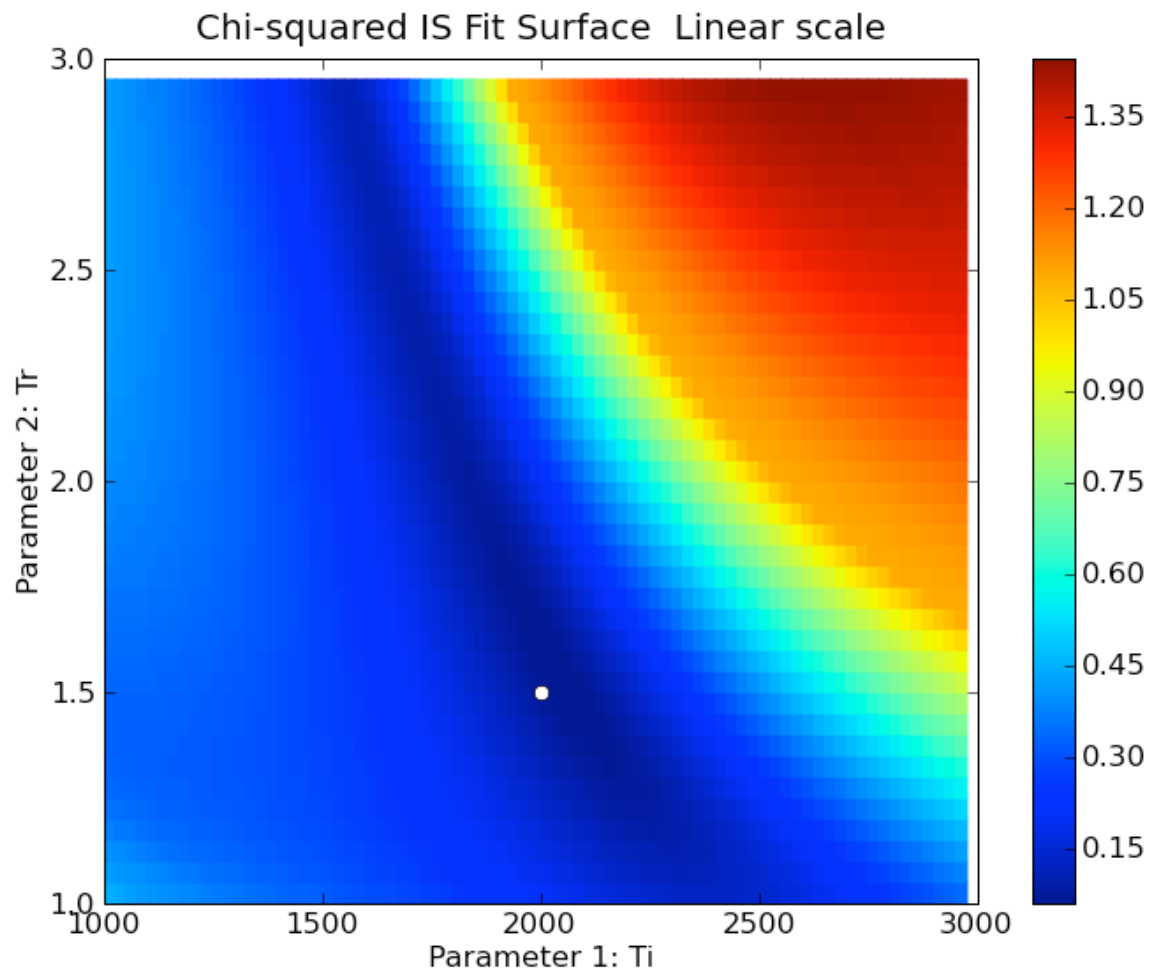
440 MHz IS Spectrum
 Ti/Tr space
 Ti = 2000 Tr = 1.5
 No noise



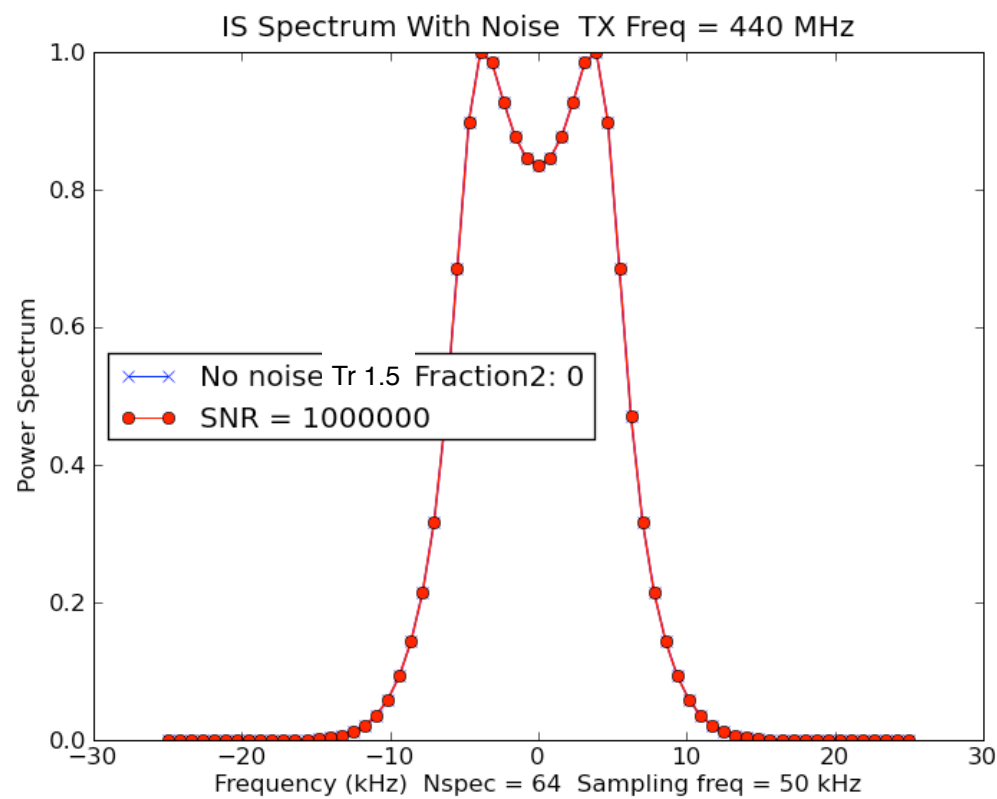
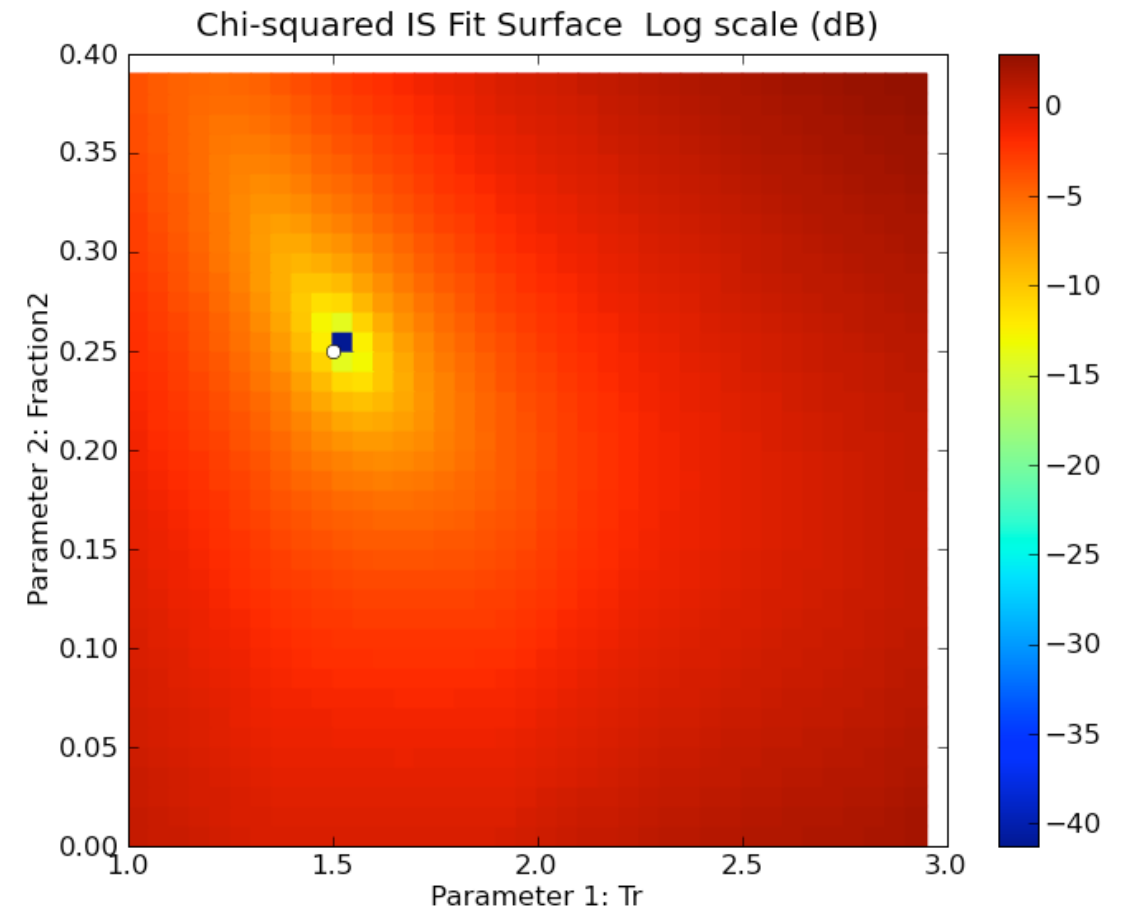
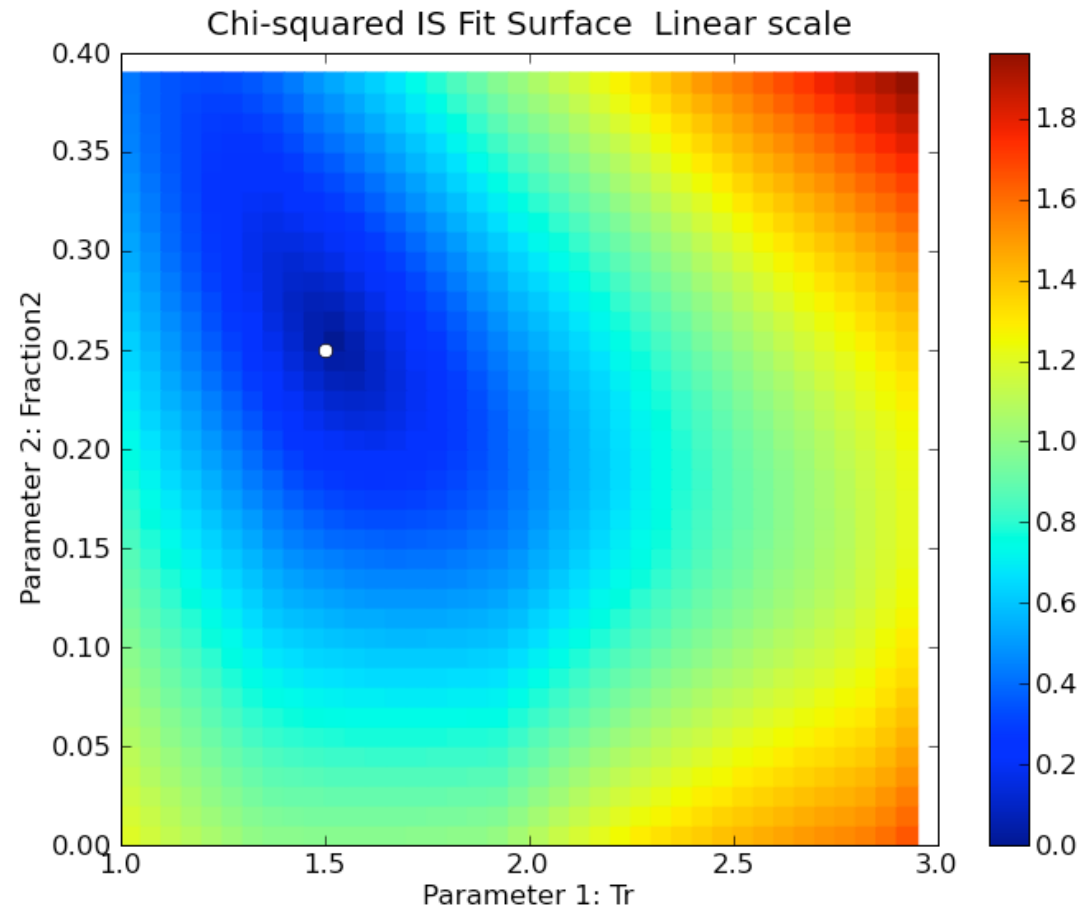
440 MHz IS Spectrum
 Ti/Tr space
 Ti = 2000 Tr = 1.5
 Poor sampling



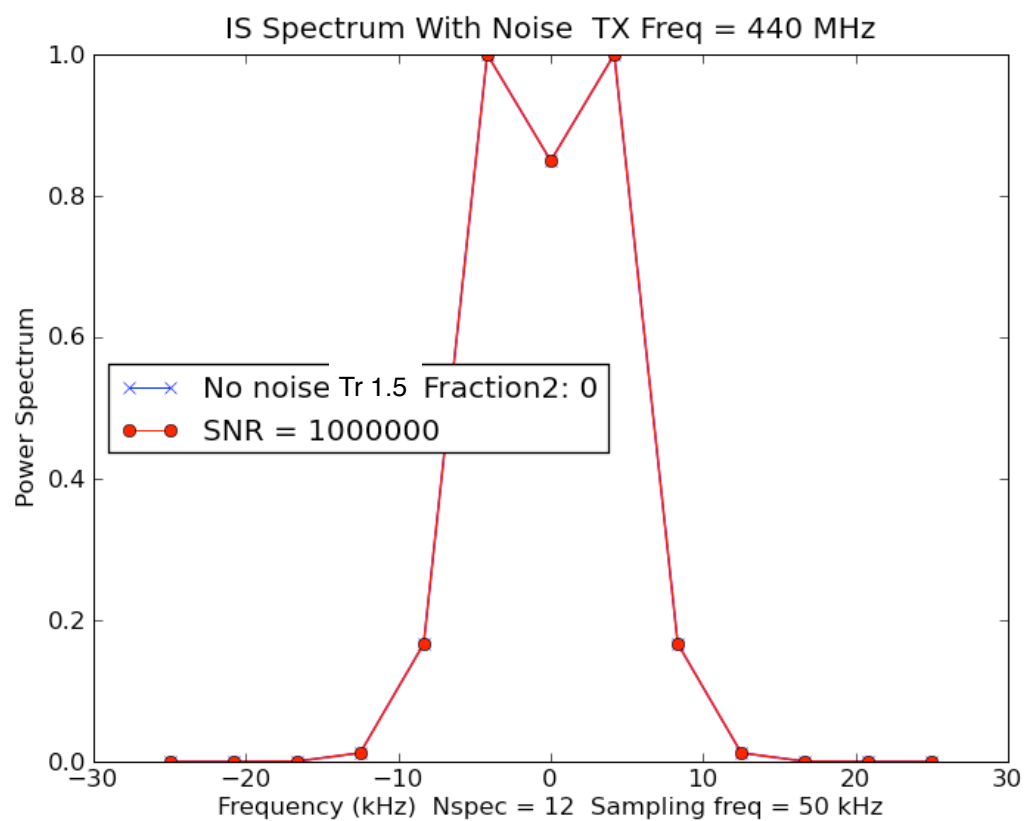
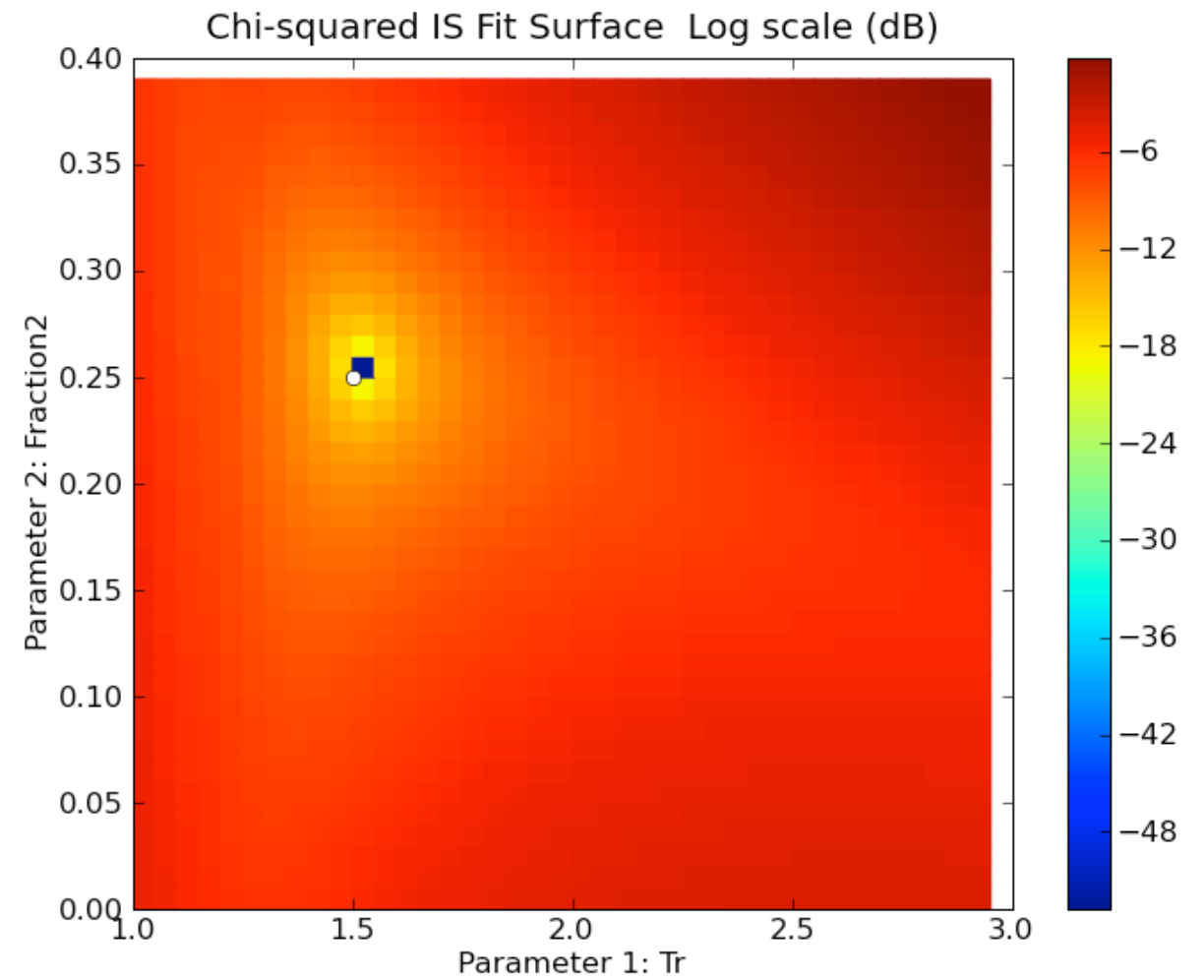
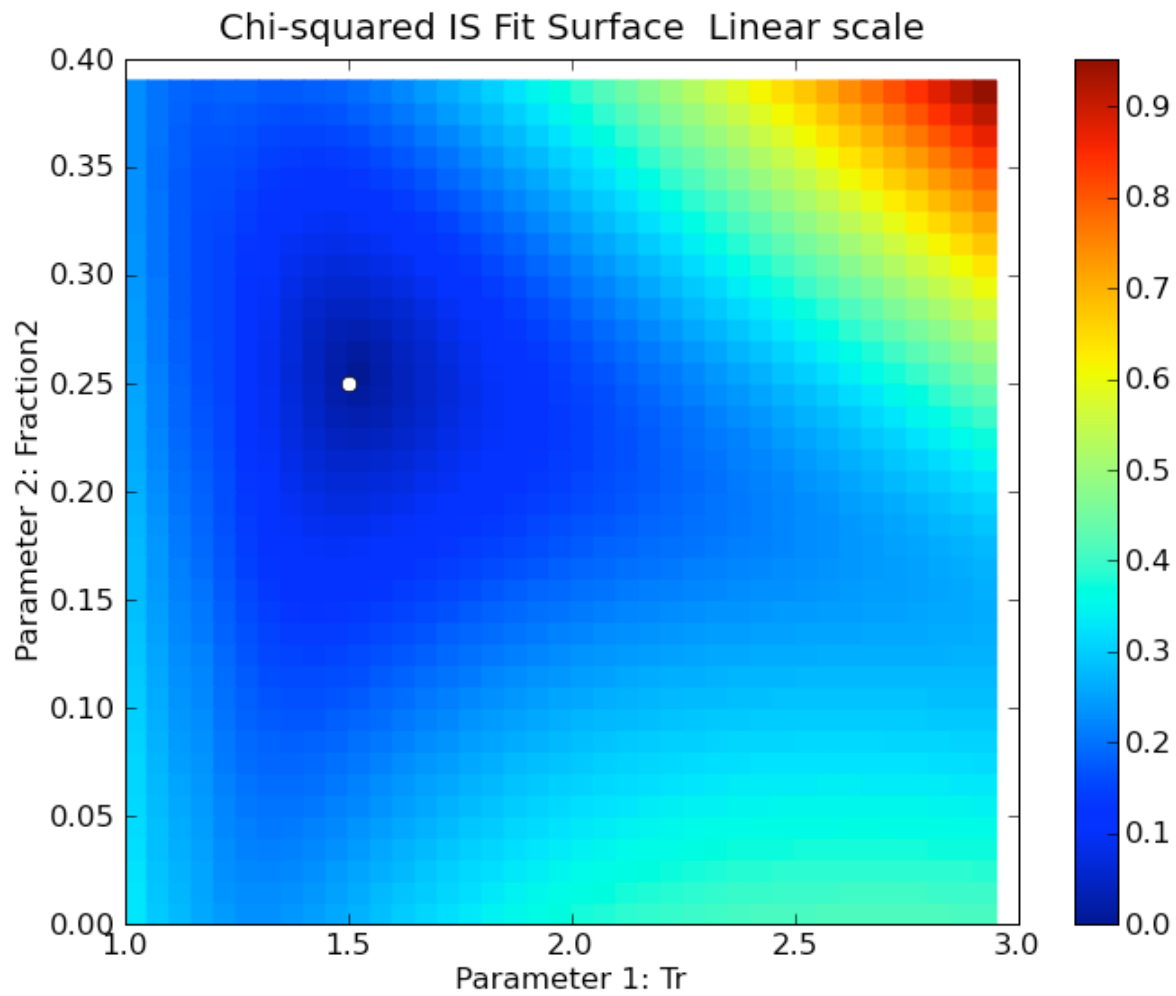
440 MHz IS Spectrum
 Ti/Tr space
 Ti = 2000 Tr = 1.5
 Noisy



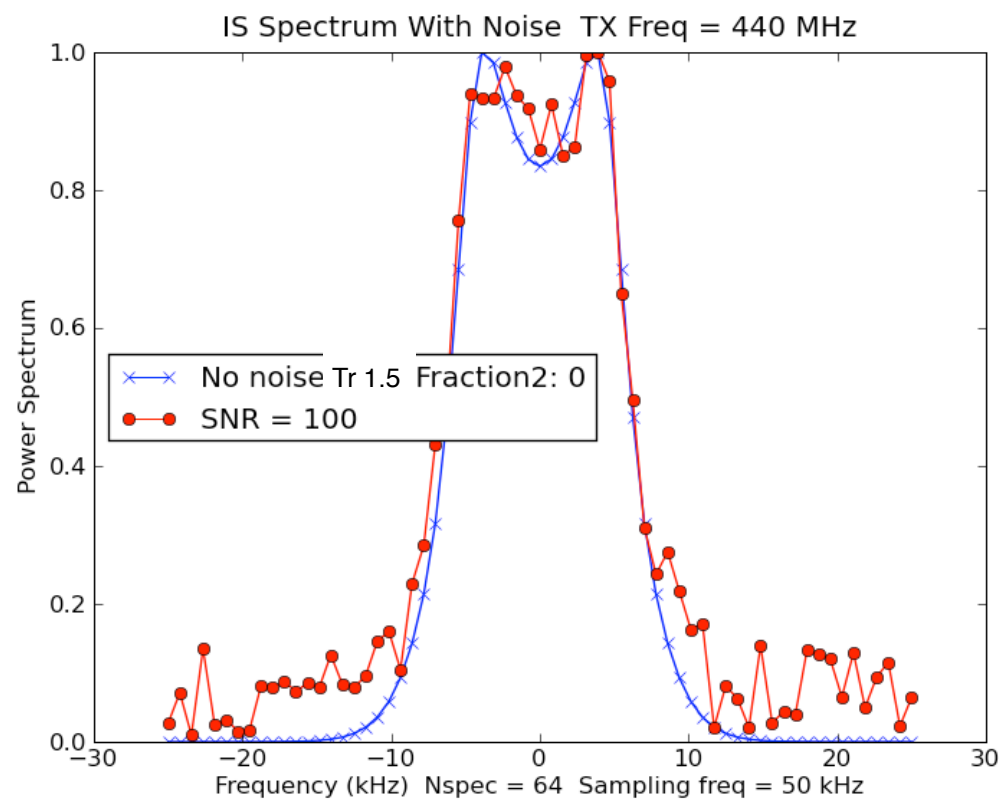
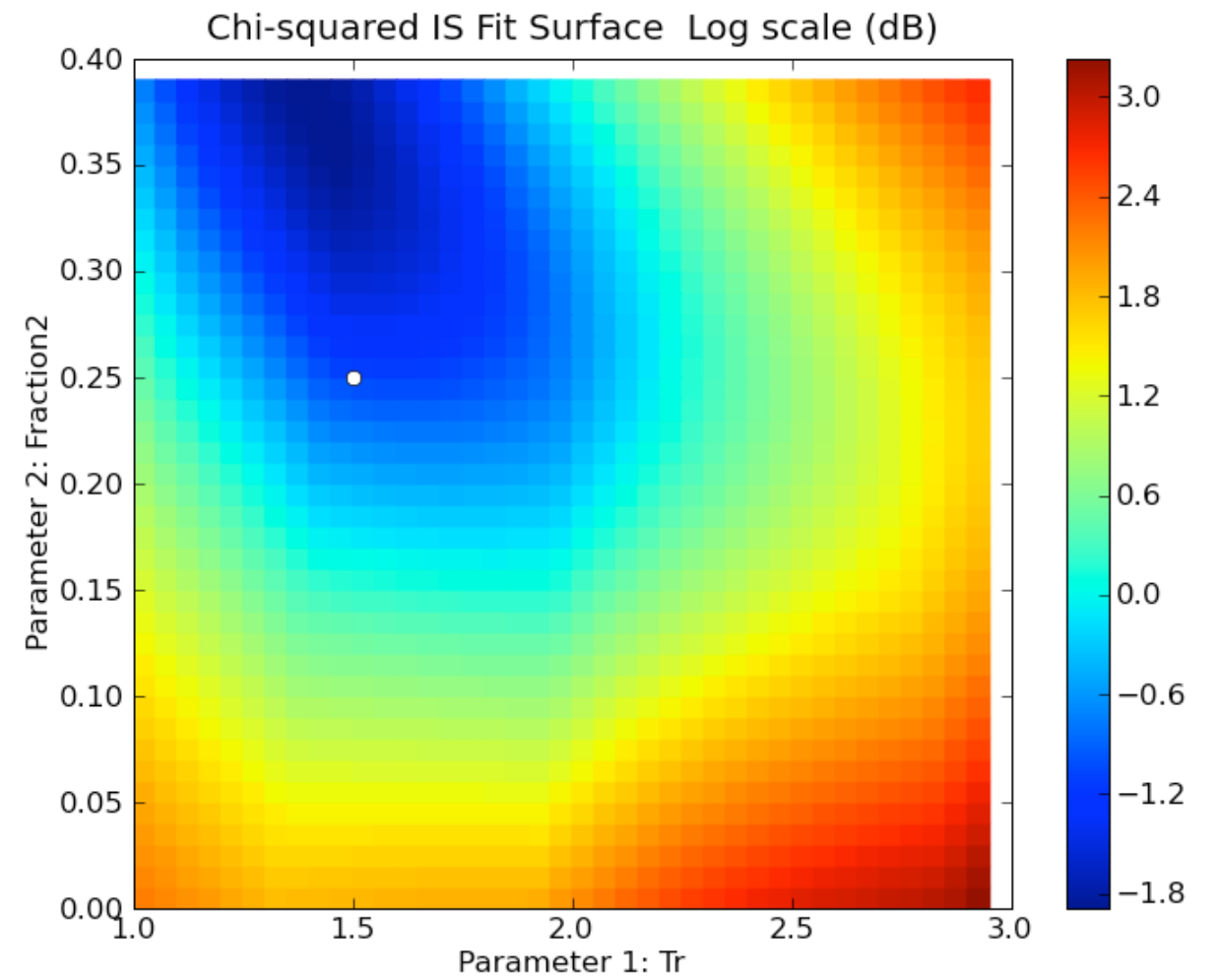
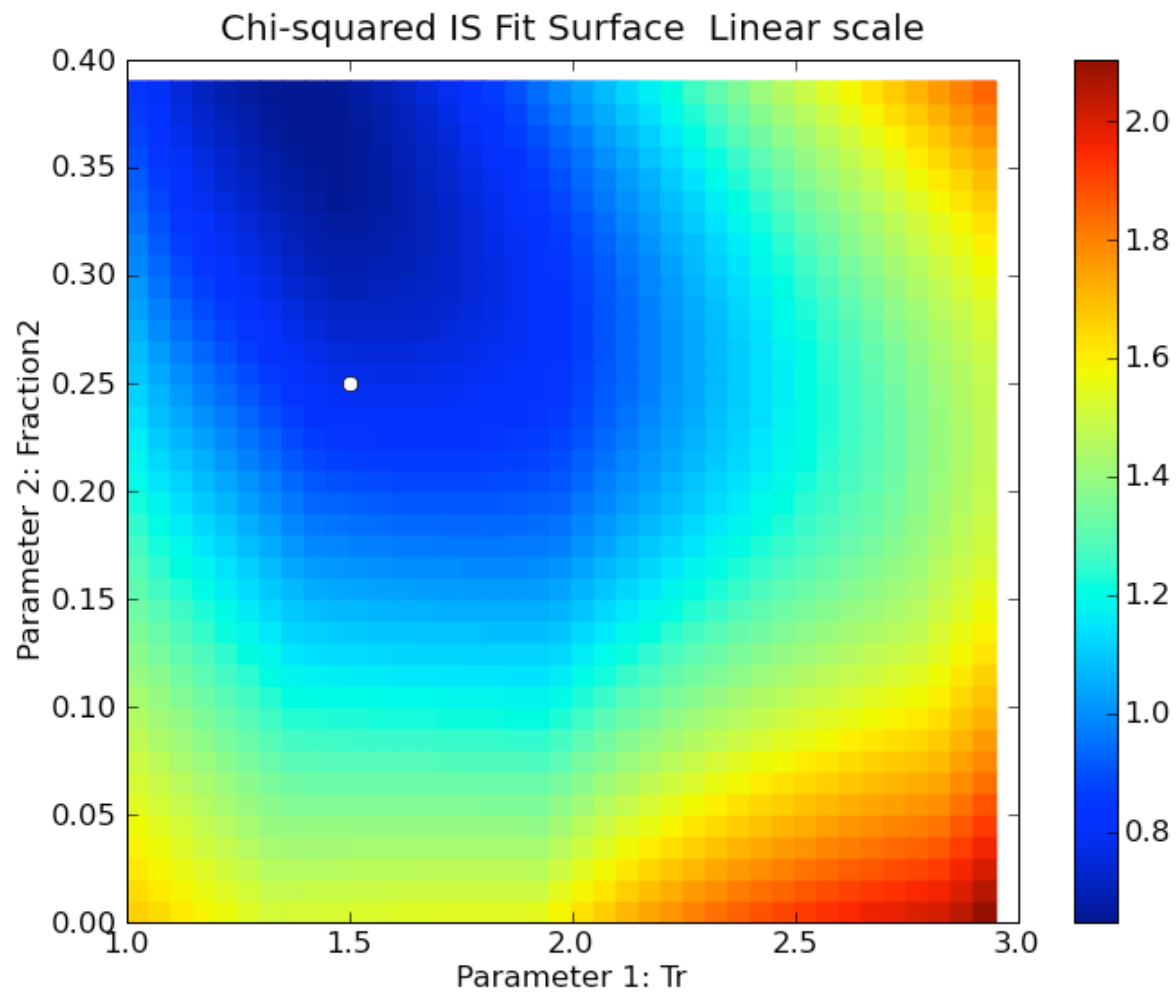
440 MHz IS Spectrum
 Ti/Tr space
 Ti = 2000 Tr = 1.5
 Noisy, poor sampling



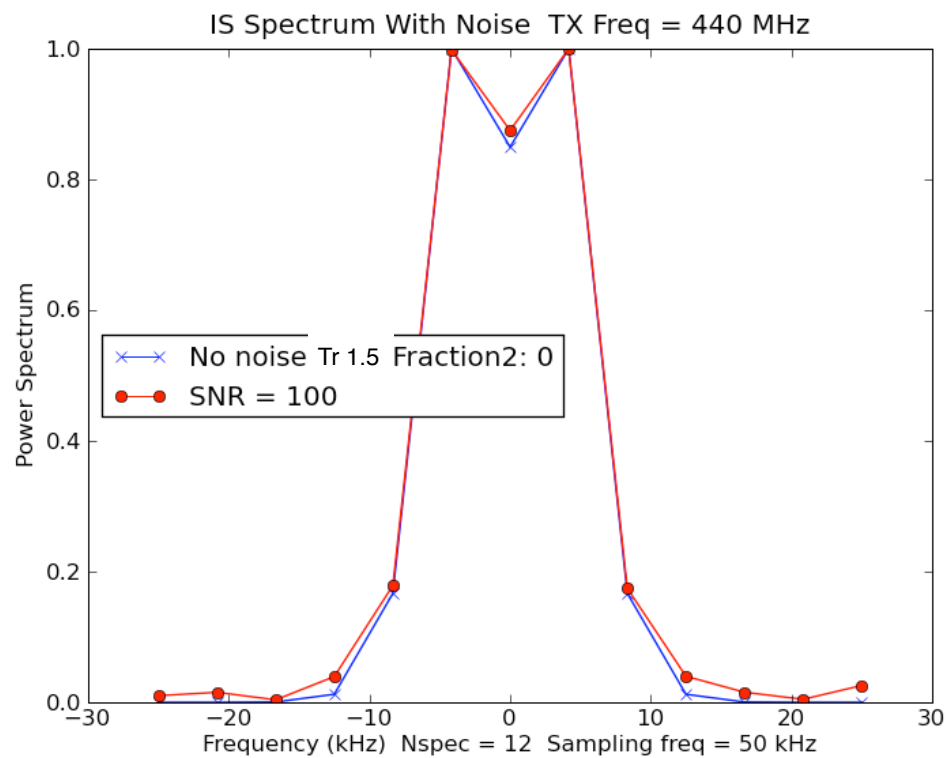
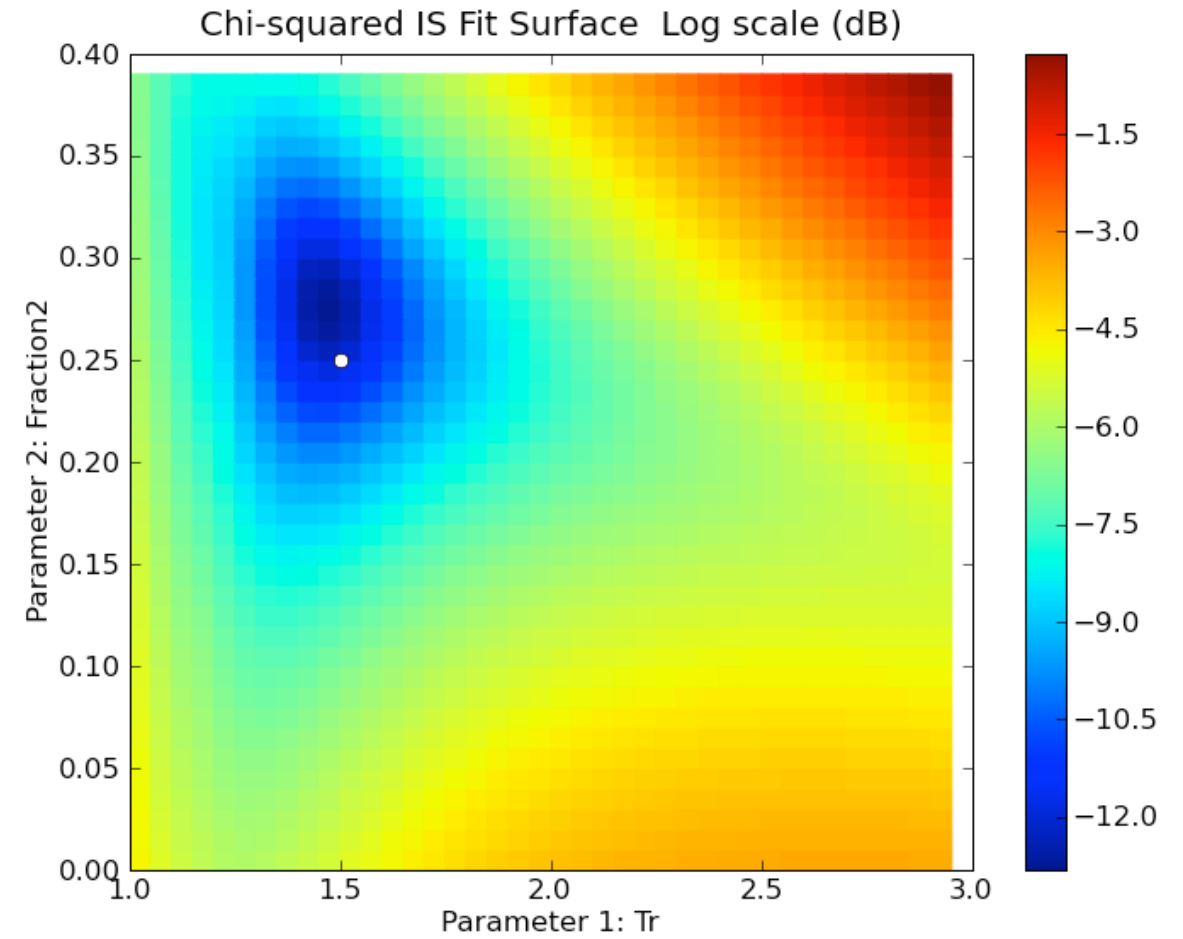
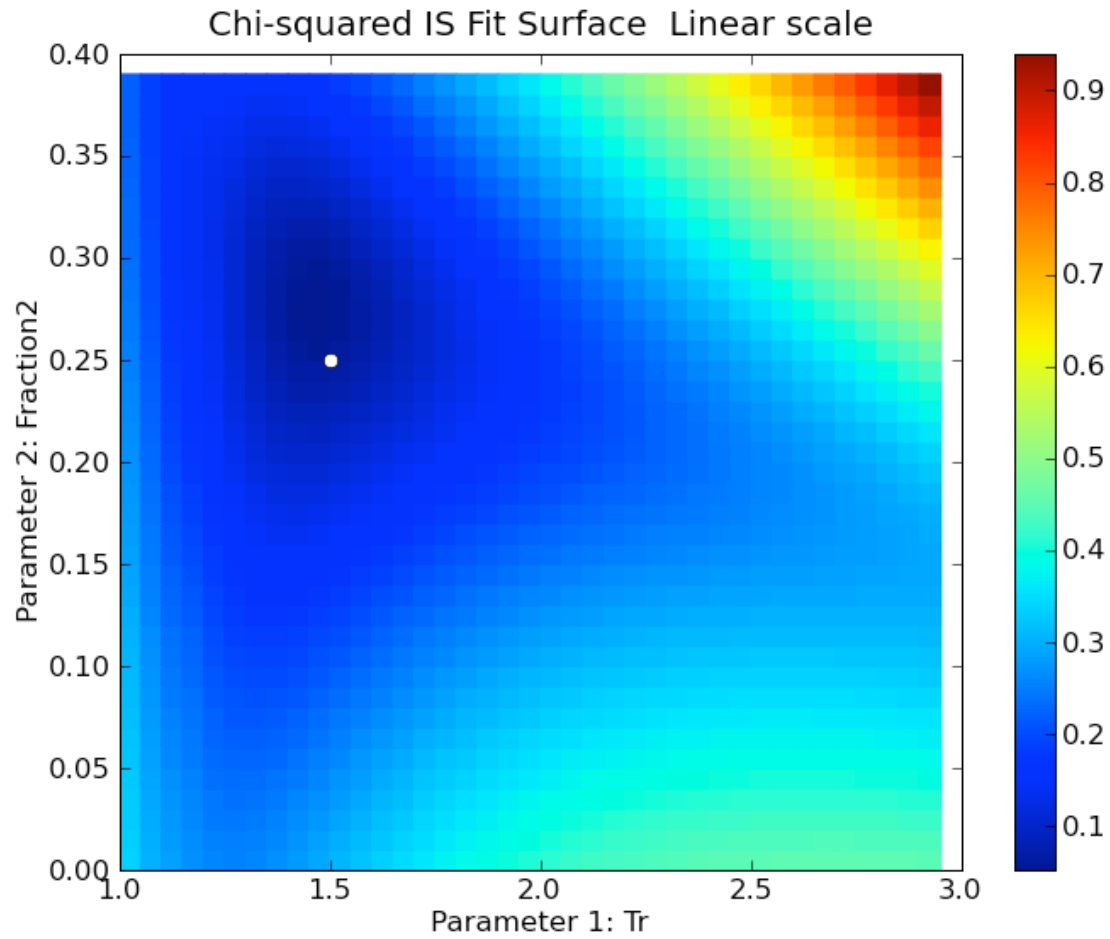
440 MHz IS Spectrum
 Tr / frac [He⁺] space
 Tr = 1.5 Ti = 1000 O⁺/He⁺ mix
 frac[He⁺]=0.25
 No noise



440 MHz IS Spectrum
 Tr / frac [He⁺] space
 Tr = 1.5 Ti = 1000 O⁺/He⁺ mix
 frac[He⁺]=0.25
 Poor sampling

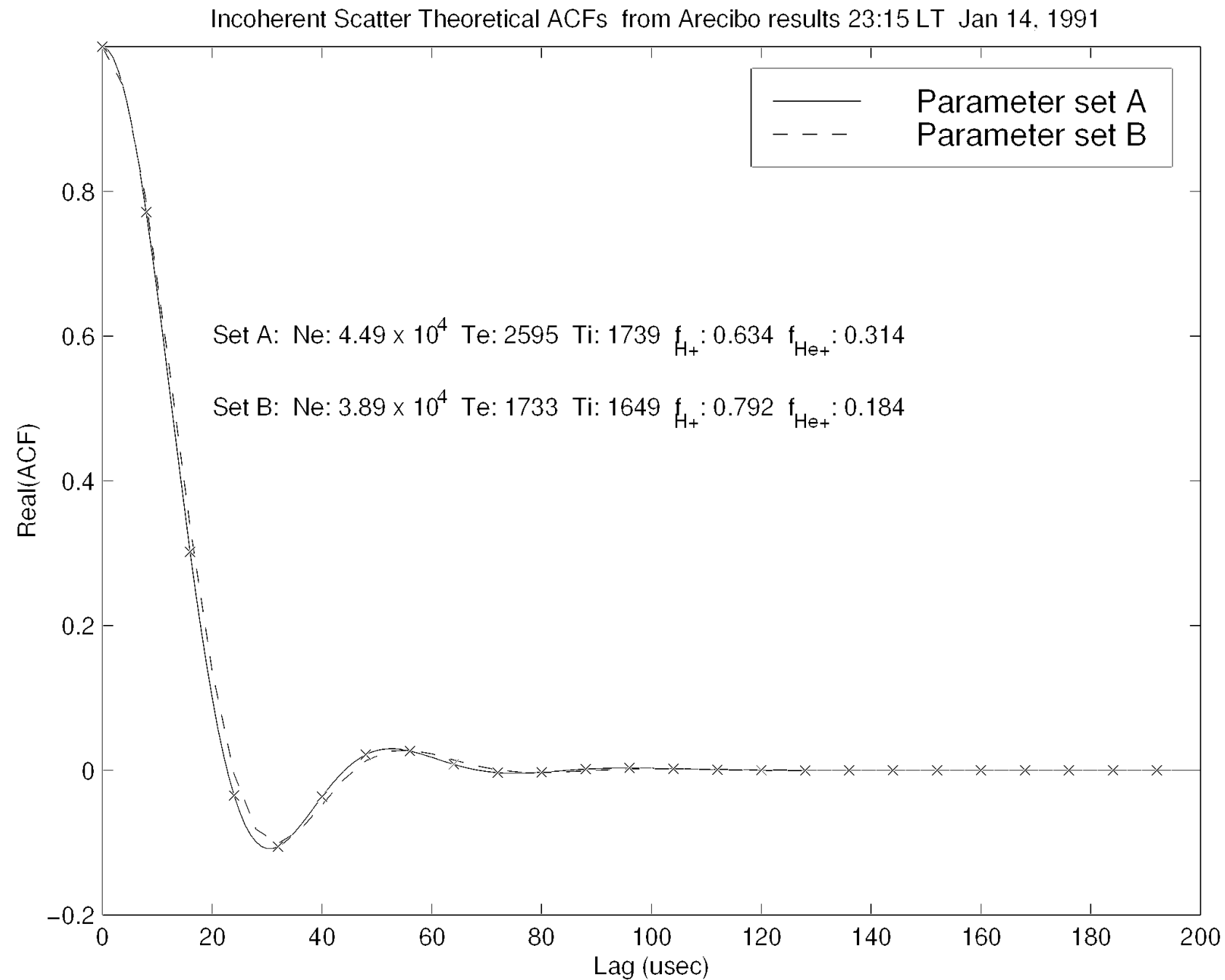


440 MHz IS Spectrum
 Tr / frac [He⁺] space
 Tr = 1.5 Ti = 1000 O⁺/He⁺ mix
 frac[He⁺]=0.25
 Noisy



440 MHz IS Spectrum
 Tr / frac [He⁺] space
 Tr = 1.5 Ti = 1000 O⁺/He⁺ mix
 frac[He⁺]=0.25
 Poor sampling, noisy

Arecibo Topside: O⁺/H⁺/He⁺/Te/Ti ambiguity



Eigenvalues of Hessian matrix (2nd derivative of min fn) has insights on parameter ambiguities

(from Roger's slides)

Table 5.1: Fit results and uncertainty values at 923 km for conditions over Arecibo at 20:41 LT on January 14, 1991. The most ill-defined parameter vector is found from the Hessian matrix eigenvector with the smallest eigenvalue.

Fitter results:

	Best-fit results	Uncertainty
N_e	6.41×10^4	7.39×10^3
T_e	2285	41.3
T_i	2223	23.4
f_{H^+}	0.490	0.00483
f_{He^+}	0.159	0.00341

Correlations between pairs of parameters:

Param Pair	Correlation	Param Pair	Correlation
$[N_e, T_e]$	0.958	$[T_e, f_{H^+}]$	-0.916
$[N_e, T_i]$	-0.649	$[T_e, f_{He^+}]$	-0.401
$[N_e, f_{H^+}]$	-0.849	$[T_i, f_{H^+}]$	0.414
$[N_e, f_{He^+}]$	-0.511	$[T_i, f_{He^+}]$	0.515
$[T_e, T_i]$	-0.440	$[f_{H^+}, f_{He^+}]$	0.099

Most ill-defined parameter combination:

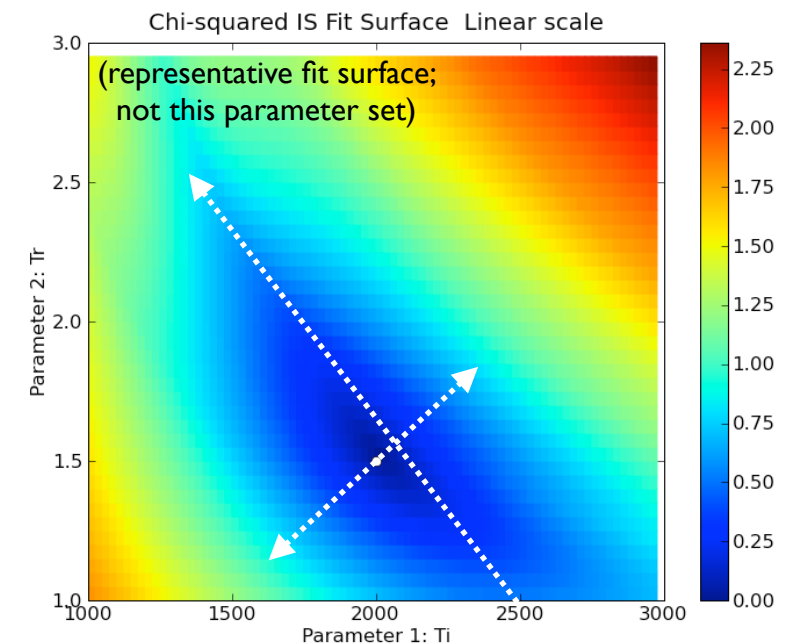
$$+0.998 (N_e) + 0.0527 (T_e) - 0.0202 (T_i) + 5.46 \times 10^{-6} (f_{H^+}) - 2.32 \times 10^{-6} (f_{He^+})$$

$$\hat{\beta}_{LS} = \min_{\beta} \sum_i \frac{[h_i(\beta) - Z_i]^2}{\sigma_i^2}$$

$$\text{Cov} \{ \hat{\beta}_{LS} \} \approx [\tilde{J}^T \tilde{J}]^{-1}$$

$$\tilde{J} = \begin{pmatrix} \frac{1}{\sigma_0} \frac{\partial h_0}{\partial \beta_0} & \frac{1}{\sigma_0} \frac{\partial h_0}{\partial \beta_1} & \dots & \frac{1}{\sigma_0} \frac{\partial h_0}{\partial \beta_{M-1}} \\ \frac{1}{\sigma_1} \frac{\partial h_1}{\partial \beta_0} & \frac{1}{\sigma_1} \frac{\partial h_1}{\partial \beta_1} & \dots & \frac{1}{\sigma_1} \frac{\partial h_1}{\partial \beta_{M-1}} \\ \vdots & \vdots & \vdots & \vdots \\ \frac{1}{\sigma_{N-1}} \frac{\partial h_{N-1}}{\partial \beta_0} & \frac{1}{\sigma_{N-1}} \frac{\partial h_{N-1}}{\partial \beta_1} & \dots & \frac{1}{\sigma_{N-1}} \frac{\partial h_{N-1}}{\partial \beta_{M-1}} \end{pmatrix}$$

Eigenvalues of $[\tilde{J}^T \tilde{J}]$



Improving the fit: adding constraints

Bayesian statistics: add apriori knowledge to stabilize fit.

Can come from other instruments, or from data at other altitudes/times.

One formulation: minimize

$$\chi^2 = \chi_{data}^2 + \chi_{apriori}^2$$

Here, the apriori information adds a cost for solutions which wander too far from the apriori knowledge. (DANGER!)

Many implementations in our field:

Constrained temperature profiles

Vector velocity fits

Full profile analysis

Regularization

Etc.

Unconstrained Arecibo topside analysis

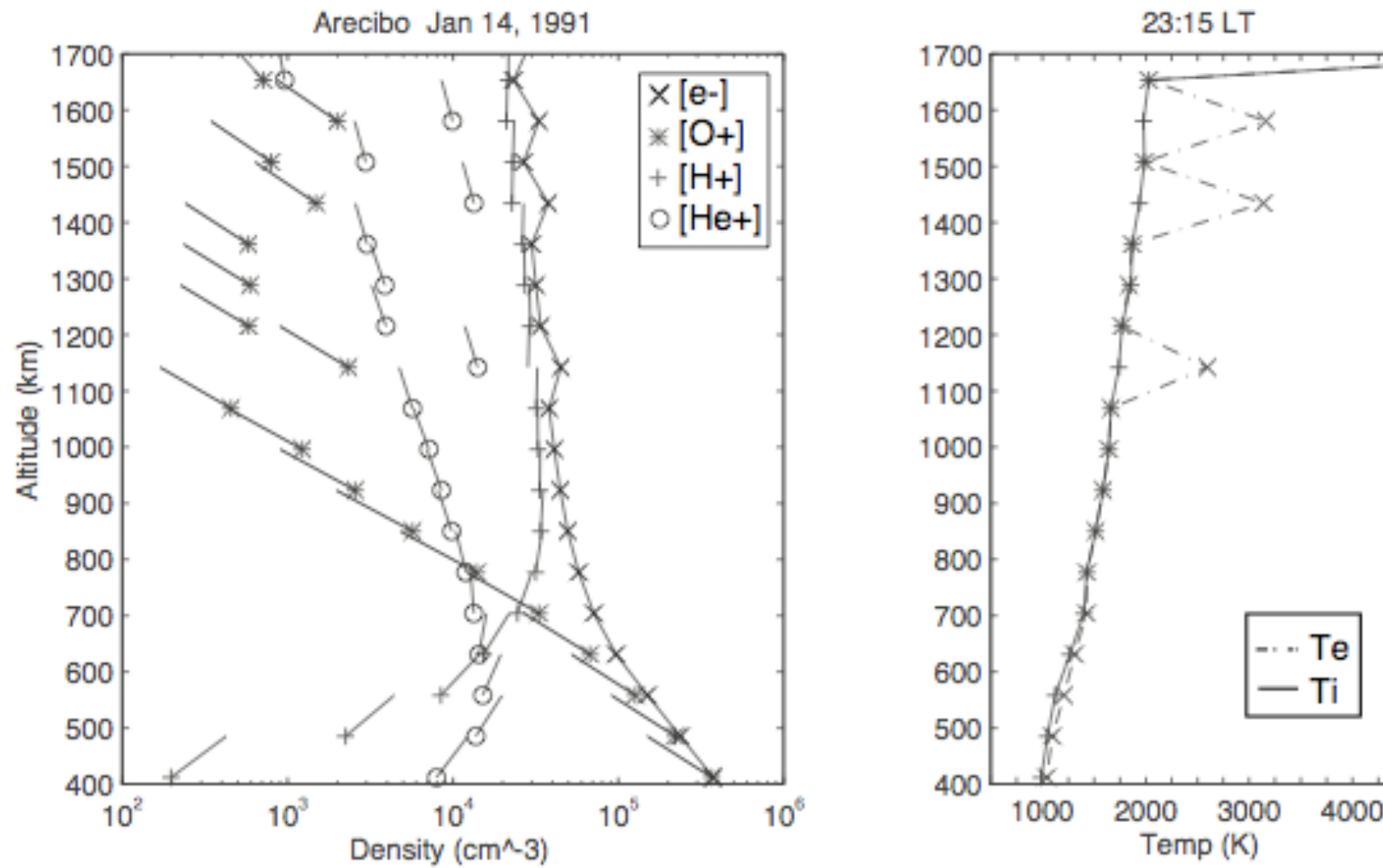


Figure 5.3: Density and temperature values as a function of altitude over Arecibo at 23:15 LT on January 14, 1991, using a 15 minute integration period. The lines emanating from each density value plotted in the left hand panel are predictions of density variation based on multicomponent diffusive equilibrium. There are clear inconsistencies in parameter values at several altitudes.

Erickson and Swartz, 1995;
Erickson, 1998

Constrained Arecibo topside analysis: Temperature gradient restriction

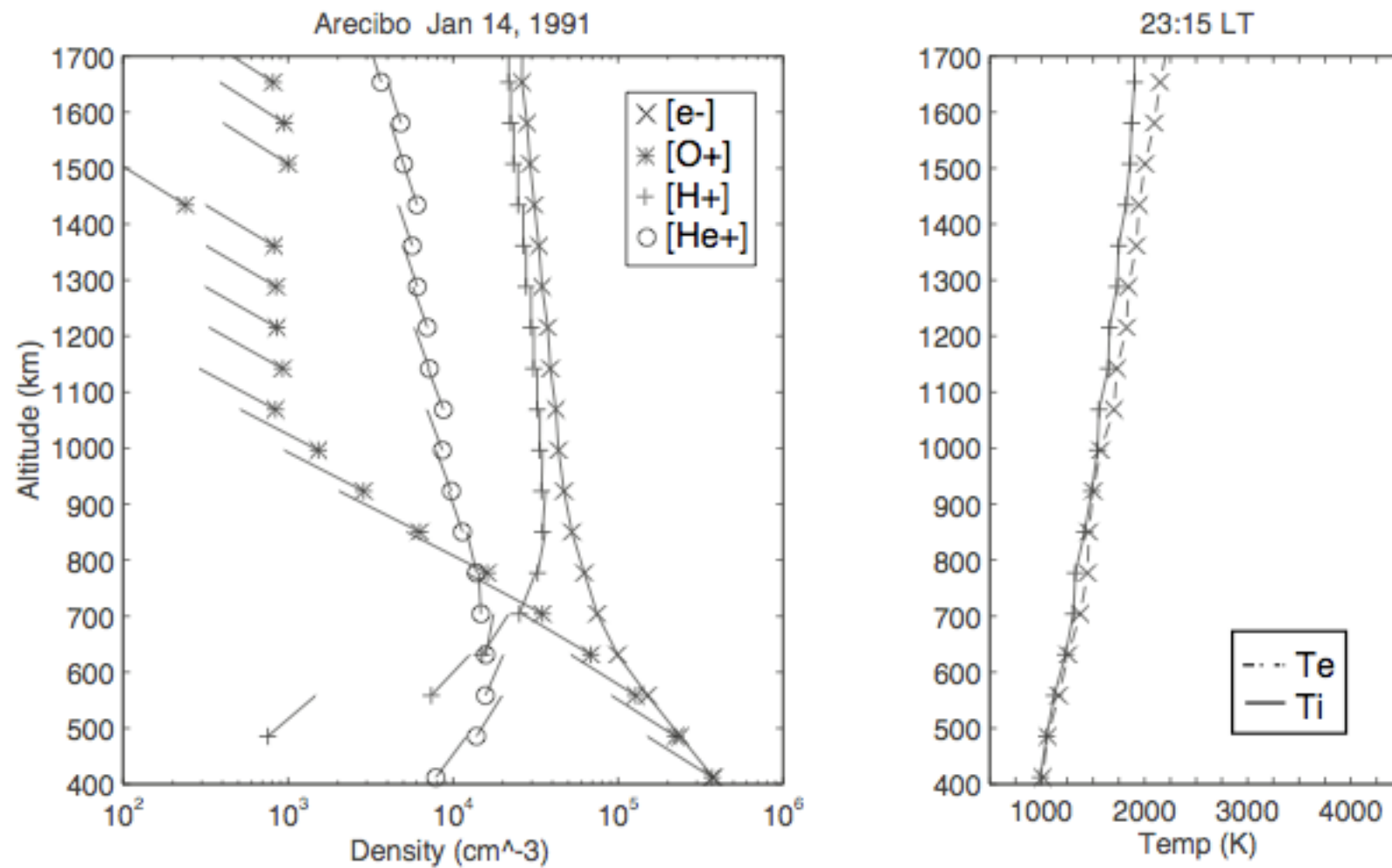


Figure 5.5: Density and temperature values as a function of altitude over Arecibo at 23:15 LT on January 14, 1991, using a 15 minute integration period. The lines emanating from each density value plotted in the left hand panel are predictions of density variation based on multicomponent diffusive equilibrium. The smooth temperature constraint results in a consistent set of fitted parameters.

Erickson and Swartz, 1995;
Erickson, 1998

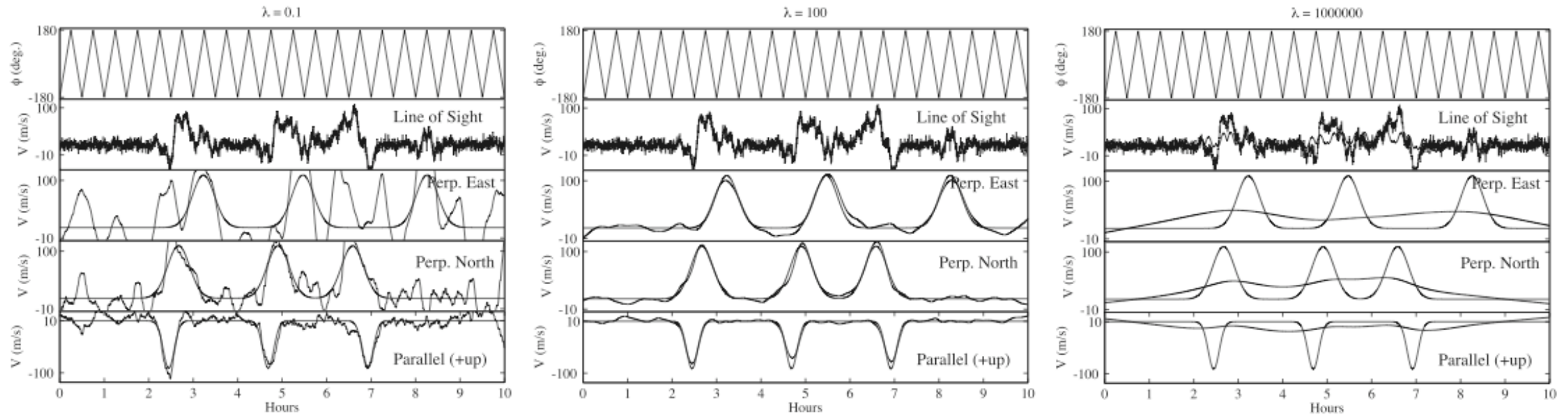


Figure 3. Vector velocity input-output comparison using a simulation assuming a single beam and applying the method of regularization. The panels on the left show the results for a small value of λ . The panels on the center were obtained from a simulation with an optimal value of λ , while the panels on the right correspond to a case with too much λ .

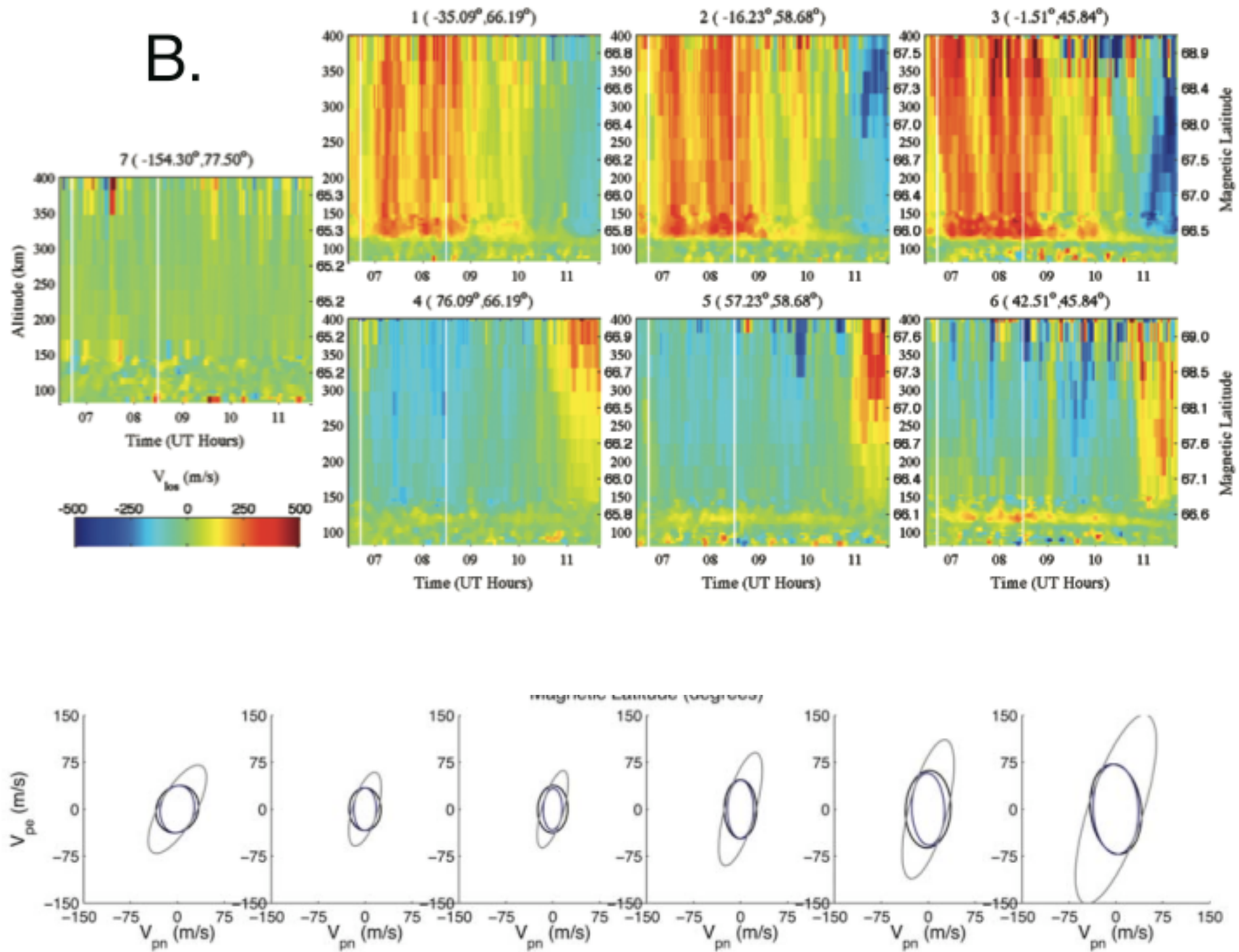
$$\begin{bmatrix} V_{pn} \\ V_{pe} \\ V_{par} \end{bmatrix} = \begin{bmatrix} -\cos \delta \sin I & \sin \delta \sin I & \cos I \\ \sin \delta & \cos \delta & 0 \\ \cos \delta \cos I & -\sin \delta \cos I & \sin I \end{bmatrix} \begin{bmatrix} v_x \\ v_y \\ v_z \end{bmatrix}.$$

$$\begin{bmatrix} V_{LOS(1)} \\ \vdots \\ V_{LOS(n)} \end{bmatrix} = \begin{bmatrix} -\cos \phi_1 \sin \theta & \sin \phi_1 \sin \theta & \cos \theta \\ \vdots & \vdots & \vdots \\ -\cos \phi_n \sin \theta & \sin \phi_n \sin \theta & \cos \theta \end{bmatrix} \begin{bmatrix} v_x \\ v_y \\ v_z \end{bmatrix}$$

Arecibo linear regularization of line-of-sight velocities for full vector derivation

Sulzer et al, 2005

Poker Flat ISR E region winds, electric fields (covariances included)



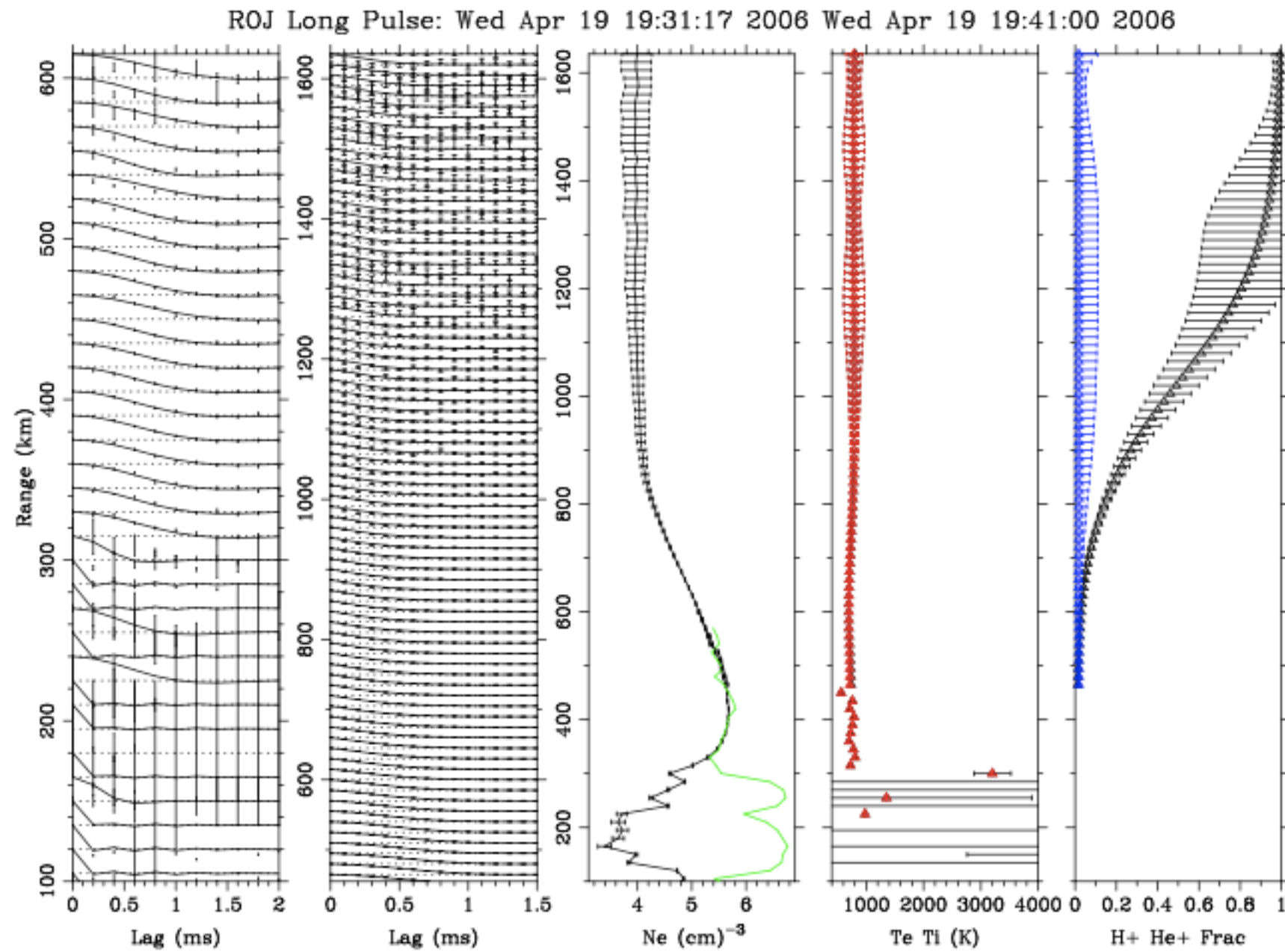


Fig. 3. Jicamarca profiles for 19:30 LT (00:30 UT). From left to right, the panels represent double-pulse lag products, long-pulse lag products, electron density, electron and ion temperature, and light ion fraction (see text).

Full profile at JRO Hysell et al, 2008
6 cost functions inject weighted apriori information